GROUNDING VIDEO MODELS TO ACTIONS THROUGH GOAL CONDITIONED EXPLORATION

Anonymous authors
Paper under double-blind review

ABSTRACT

Large video models, pretrained on massive quantities of amount of Internet video, provide a rich source of physical knowledge about the dynamics and motions of objects and tasks. However, video models are not grounded in the embodiment of an agent, and do not describe how to actuate the world to reach the visual states depicted in a video. To tackle this problem, current methods use a separate vision-based inverse dynamic model trained on embodiment-specific data to map image states to actions. Gathering data to train such a model is often expensive and challenging, and this model is limited to visual settings similar to the ones in which data is available. In this paper, we investigate how to directly ground video models to continuous actions through self-exploration in the embodied environment – using generated video states as visual goals for exploration. We propose a framework that uses trajectory level action generation in combination with video guidance to enable an agent to solve complex tasks without any external supervision, e.g., rewards, action labels, or segmentation masks. We validate the proposed approach on 8 tasks in Libero, 6 tasks in MetaWorld, 4 tasks in Calvin, and 12 tasks in iThor Visual Navigation. We show how our approach is on par with or even surpasses multiple behavior cloning baselines trained on expert demonstrations while without requiring any action annotations. Results are best viewed on our website: https://sites.google.com/view/video-to-actions.

1 INTRODUCTION

Large video models (Brooks et al., 2024; Girdhar et al., 2023; Ho et al., 2022) trained on a massive amount of Internet video data capture rich information about the visual dynamics and semantics of the world for physical decision-making. Such models are able to provide information on how to accomplish tasks, allowing them to parameterize policies for solving many tasks (Du et al., 2024). They are further able to serve as visual simulators of the world, allowing simulation of the visual state after a sequence of actions (Brooks et al., 2024; Yang et al., 2024c), and enabling visual planning to solve long-horizon tasks (Du et al., 2023).

However, directly applying video models zero-shot for physical decision-making is challenging due to embodiment grounding. While generated videos provide a rich set of visual goals for solving new tasks, they do not explicitly provide actionable information on how to reach each visual goal. To ground video models to actions, existing work has relied on training an inverse dynamics model or goal-conditioned policy on a set of demonstrations from the environment (Black et al., 2023; Du et al., 2024; 2023). Such an approach first requires demonstrations to be gathered in the target environment and embodiment of interest, which demands human labor or specific engineering (e.g. teleoperation or scripted policy). In addition, the learned policies may not generalize well to areas in an environment that are out-of-distribution of training data.

Recently, (Ko et al., 2023) proposes an approach to directly regress actions from video models, without requiring any action annotations. In (Ko et al., 2023), optical flow between synthesized video frames is computed and used, in combination with a depth map of the first image, to compute a rigid transform of objects in the environment. Robot actions are then inferred by solving for actions that can apply the specified rigid transform on an object. While such an approach is effective on a set of evaluated environments, it is limited in action resolution as the inferred object transforms can be imprecise due to both inaccurate optical flow and depth, leading to a relatively low success rate in

evaluated environments (Ko et al., 2023). In addition, it is difficult to apply this approach to many robotic manipulation settings such as deformable object manipulation, where there are no explicit object transforms to compute.

We propose an alternative manner to directly ground a video model to actions *without using annotated demonstrations*. In our approach, we learn a goal-conditioned policy, which predicts the actions to reach each synthesized frame in a video. We learn the policy in an online manner, where given a specified task, we use each intermediate synthesized frame as a visual goal for a goal-conditioned policy from which we obtain a sequence of actions to execute in an environment. We then use the image observations obtained from execution in the environment as ground-truth data to train our goal-conditioned policy. We illustrate our approach in Figure 1.

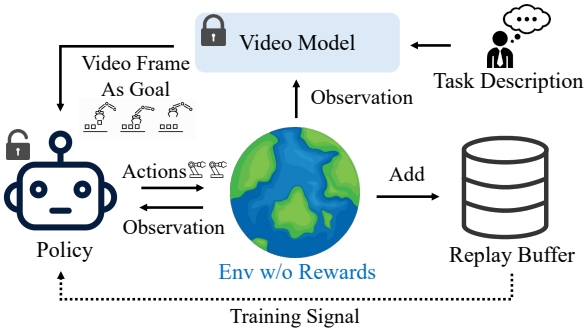

Figure 1: **Grounding Video Model to Actions.** Our approach learns to ground a large pretrained video model into continuous actions through goal-directed exploration in an environment. Given a synthesized video, a goal-conditioned policy attempts to reach each visual goal in the video, with data in the resulting real-world execution saved in a replay buffer to train the goal-conditioned policy.

In practice, directly using synthesized images as goals for exploration often leads to insufficient exploration. Agents often get stuck in particular parts of an environment, preventing the construction of a robust goal-conditioned policy. To further improve exploration, we propose to generate chunks of actions to execute in an environment given a single visual state. By synthesizing and executing a chunk of actions we can explore the environment in a more directed manner, enabling us to achieve a more diverse set of states. We further intermix goal-conditioned exploration with random exploration to further improve exploration.

Overall, our approach has three contributions: **(1)** We propose goal-conditioned exploration as an approach to ground video models to continuous actions. **(2)** We propose a set of methods to enable robust exploration in an environment to learn a robust goal-conditioned policy, using chunked action prediction and exploration with periodic randomized exploration. **(3)** We illustrate the efficacy of our approach on a set of simulated manipulation and navigation environments.

2 Related Work

Video Model in Decision making A large body of recent work has explored how video models can be used in decision making (Yang et al., 2024d; McCarthy et al., 2024). Prior work has explored how video models can act as reward functions (Escontrela et al., 2024; Huang et al., 2023; Chen et al., 2021), representation learning (Seo et al., 2022; Wu et al., 2023; 2024; Yang et al., 2024b), policies (Ajay et al., 2024; Du et al., 2024; Liang et al., 2024), dynamics models (Yang et al., 2024c; Du et al., 2024; Zhou et al., 2024b; Brooks et al., 2024; Rybkin et al., 2018; Mendonca et al., 2023), and environments (Bruce et al., 2024). Our work explores that given video generations, how we can learn a policy and infer the actions to execute in an environment *without any action labels*, while existing works (Baker et al., 2022; Bharadhwaj et al., 2024a; Black et al., 2023; Wen et al., 2023; Zhou et al., 2024a; Wang et al., 2024) requires domain specific action data. Most similar to our work is AVDC (Ko et al., 2023), which uses rigid object transformations computed by optical flow between video frames as an approach to extract actions from generated videos. We propose an alternative unsupervised approach to ground video models to continuous action by leveraging video-guided goal-conditioned exploration to learn a goal-conditioned policy.

Learning from Demonstration without Actions. A flurry of work has studied the problem of robot learning from demonstrations without actions. One line of work studies the problem of extrapolating the control actions assuming that the expert state trajectories are provided (Torabi et al., 2018; Radosavovic et al., 2021; Li et al., 2024), though collecting such ground-truth state-level data is expensive and hard to scale. Some recent work explores learning from image/video robotic data without actions (Seo et al., 2022; Wu et al., 2024; Mendonca et al., 2023; Ma et al., 2022; Wang et al., 2023; Ma et al., 2023; Schmeckpeper et al., 2021), either by constructing a world model, reward model, or representation model. However, these methods usually need additional finetuning

on data or rewards from specific downstream environments. By contrast, our method uses action-free demonstration videos to train a video generative model and leverages the generated frames as goals to learn a goal-conditioned policy to complete a task. As a result, our policy learning requires neither action labels or environment awards which can be challenging to obtain.

Robotic Skill Exploration. Typical robot skill exploration is formulated as an RL problem (Haarnoja et al., 2018; Hafner et al., 2019) and assumes some form of environment rewards, but the design of reward functions is highly task dependent and demands human labor. To this end, some recent work explores robotic skill exploration without any rewards. One typical class of methods is developed upon computing intrinsic exploration rewards to promote rare state visit. These methods can be based on prediction error maximization (Pathak et al., 2017; Henaff, 2019; Shyam et al., 2019), disagreement of an ensemble of world models (Hu et al., 2022; Sekar et al., 2020; Sancaktar et al., 2022), entropy maximization (Pong et al., 2020; Pitis et al., 2020; Jain et al., 2023; Eysenbach et al., 2019), counting (Bellemare et al., 2016), or relabeling (Ghosh et al., 2021). However, discrepancy, counting, or relabeling based methods are limited to simple environment, short-horizon tasks or low-dimensional state-space. We propose to use video models for direct exploration, as large pretrained video models are a rich source of task-specific information. With efficient guidance from the video model, we show that our method is able to collect high-quality data from the environment and accomplish challenging long-horizon tasks conditioned on language instruction at test-time.

3 METHOD

In this section, we describe our method to ground video model to actions by unsupervised exploration in the environments. First, in Section 3.1, we describe the pipeline of policy execution conditioned on video frame and hindsight relabeling via environment rollouts. Next, we introduce a periodic random action bootstrapping technique to secure the quality of video-guided exploration in Section 3.2. Finally, in Section 3.3, we propose a chunk-level action prediction technique to further enhance the coverage, stability, and accuracy of the goal-conditioned policy. The pseudocode of our method is provided in Algorithm 1.

3.1 LEARNING GOAL-CONDITIONED POLICIES THROUGH VIDEO-GUIDANCE AND HINDSIGHT RELABELING

A key challenge in unsupervised skill exploration is that the possible underlying environment states are enormous, making it difficult for an agent to discover and be trained on every valid state, especially in the high-dimensional visual domain. Many relevant states for downstream task completion, such as stacking blocks on top of each other or opening a cabinet, require a very precise sequence of actions to obtain, which is unlikely to happen from random exploration.

Video models have emerged as a powerful source of prior knowledge about the world, providing rich information about how to complete various tasks from large-scale internet data. We leverage the knowledge contained in these models to help guide our exploration in an environment to solve new tasks. To this end, we propose a novel method that uses a pre-trained video model $f_\theta(x_{\text{start}}, c)$ to guide the exploration and shrink the search space only to task-relevant states (x_{start} denote the initial observation and c denote the corresponding task description). This concurrently benefits both sides: the goal-conditioned policy obtains task-relevant goals so as can perform efficient exploration centered around the task-relevant state space; on the other hand, the underlying information from the video model is extracted to end effectors and enables effective decision-making and control in embodied agents. Specifically, during exploration, we first leverage the video model to generate a sequence of images based on the given image observation x_{start} and language task description c,

$$\texttt{pred\_v} = f_\theta(x_{\text{start}}, c), \quad \text{where } x_{\text{start}} \sim \mathcal{O} \text{ and } c \sim \mathcal{T} \tag{1}$$

where $\mathcal{O}$ is the observation space and $\mathcal{T}$ is the task space. We then execute the actions predicted by the goal-conditioned policy $a^{\text{pred}} = \pi(a|x_{\text{start}}, x_{\text{goal}})$ in the environment, where the goal x_{goal} is set to each predicted video frame $\texttt{pred\_v}_i$ sequentially. Hence, we can obtain an episode of image action pairs $(x^{\text{env}}_{1:t}, a^{\text{pred}}_{1:t})$ of length t from the environment and these rollout data will be added to a replay buffer R for policy training.

At the beginning of training, these data might not necessarily reach the exact goals given by the video model, but are still effective to indicate the task-specific region, since the rollout results of $a^{\text{pred}}_{1:t}$ are relabeled and can reflect the ground-truth environment dynamics. Empirically, we observe the

Algorithm 1 Grounding Video Model to Actions

Require: a frozen video diffusion model $f_\theta(x_{\text{start}}, c)$, a goal conditioned policy to train $\pi(a|x_{\text{start}}, x_{\text{goal}})$, a replay buffer R
Hyperparameters: horizon of policy π h, training iteration N, number of initial / additional random action episodes n_r / n_r', video-guided / random action exploration frequency q_v / q_r
Sample n_r episodes of random actions and add to replay buffer R
for $i = 1 \rightarrow N$ **do**
  if $i \mod q_v == 0$ **then** *# conduct video-guided exploration with frequency q_v*
    Sample a task c', obtain observation x_0, and generate video $\texttt{pred\_v} = f_\theta(x_0, c')$
    Execute policy $\pi(a|\cdot, \cdot)$ in the environment where the goals are frames from $\texttt{pred\_v}$
    Add the resulting image-action pairs from the video rollout to replay buffer R
  end if
  if $i \mod q_r == 0$ **then** *# conduct periodic random action bootstrapping with frequency q_r*
    Sample additional n_r' episodes of random actions and add to replay buffer R
  end if
  # train the policy with the data sampled from the replay buffer
  $(x_{i:i+h}, a_{i:i+h})$ = sample a consecutive sequence of image-action pairs from replay buffer R
  $a^{\text{pred}} = \pi(a|x_i, x_{i+h})$
  $\mathcal{L} = \text{MSE}(a^{\text{pred}}, a_{i:i+h})$
end for
return goal-conditioned policy π

proposed video-guided exploration scheme is very effective, and we visualize the curve of number of success versus total number of video-guided rollouts in Figure 8. Our overall training objective is

$$\max_{\phi} \ \mathbb{E}_{(x_{i:i+h}, a_{i:i+h}) \sim R}\big[\log \pi_\phi(a_{i:i+h}|x_i, x_{i+h})\big] \tag{2}$$

where i is a randomly sampled temporal index inside a rollout episode, h denotes the horizon of the policy, and ϕ represents the parameters of the goal-conditioned policy. Note that provided a video model f_θ trained on internet scale data, the video predictions can be easily generalized to a broad observation space $\mathcal{O}$ and task space $\mathcal{T}$, enabling the proposed guidance scheme directly applied to various unseen scenarios.

3.2 Periodic Random Action Bootstrapping

When a goal-conditioned policy is initialized from scratch, it is unable to effectively process the frames provided by a video model and use them to guide exploration, as it is unable to process input frames. Empirically, we found that a randomly initialized policy would often instead preferentially output particular actions (i.e. only move up) independent of goals given by the video model.

This significantly compromises the exploration because the policy will not explore the task-related states as we expect. More importantly, though we can obtain ground-truth environment dynamics via hindsight relabeling, the actions in the replay buffer R are output from the scratch policy itself. This might result in an undesirable loop where only the previous outputs are used as the ground-truth and these actions are irrelevant to completing the task.

To this end, inspired by random action sampling in RL setting (Sutton, 2018), we propose a novel periodic random action bootstrapping method for grounding video model to actions. Specifically, we first conduct random action exploration and append the resulting data to the replay buffer R before the training starts, and periodically conduct extra random exploration during training. The process can be denoted by

$$R \ \leftarrow \ a_{1:t^r}^{i_r} \sim \texttt{Uniform}\big[a_{\text{low}}, a_{\text{high}}\big] \quad \text{for } i^r \text{ in } [1, 2, ..., n_r] \tag{3}$$

where n_r denotes the number of random action episodes, t^r denotes the length of a random action episode, a_{low} and a_{high} are the action limits. This proposed bootstrapping method can enhance the exploration in two ways: the initial random actions serve as the basic world dynamics information which enables the policy to reach the vicinity of goal states specified by video frames, ensuring effective video-guided exploration; the periodic extra random exploration can further expand the agent's discovered state space and stabilize policy training. Please see Section 4.3 for ablation studies and Appendix D.3 for implementation details.

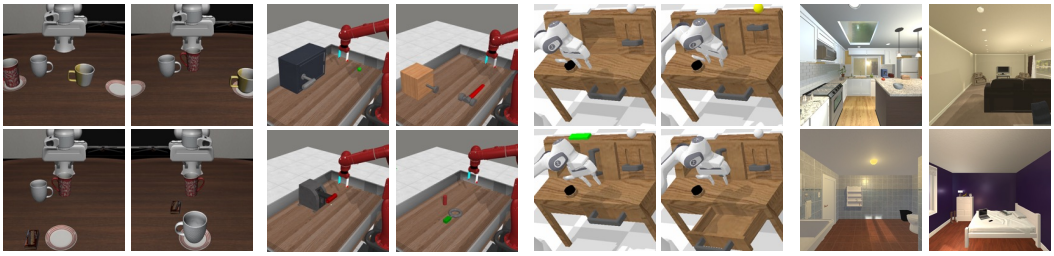

(a) Libero (b) Meta-World (c) Calvin (d) iTHOR

Figure 2: **Environment Demonstrations.** We evaluate our method on three robotic manipulation environments: Libero, Meta-World, Calvin, and one visual navigation environment: iThor, with a total of 30 tasks. Images in (a) and (c) denote the goal object states of a subset of tasks. Images in (b) are randomly sampled start observation of a subset of tasks. In (d), we show the layout for each scene in the agent's view from a specific position.

3.3 Chunk Level Action Prediction and Exploration

In current robot exploration frameworks, the policy usually predicts a single action as output and explores the environment with a single action. However, this single action method can hinder diverse exploration, as it might easily fall to a single modality or local minima, which significantly constrains the covered state space. Moreover, single action prediction does not fully leverage the data coherency and context information collected by the agent during consecutively interactions with the environment. In addition, single action exploration requires one model forward pass for each action, resulting in a larger computational burden and higher latency.

To tackle these issues, we propose to predict a sequence of actions with horizon h and explore the environments using the predicted chunks of actions. On one hand, by modeling behavior over a longer horizon, chunk-level action prediction can encourage more coherent action sequences and mitigate myopic actions and compounding error, especially when the temporal distance to the goal is large. On the other hand, exploration with action chunks can in turn collect more coherent data from the environment, further facilitating the policy to capture the underlying environment dynamics. In addition, we utilize chunk-level actions during random exploration. Specifically, we sample an action mean a^m from a uniform distribution, and based on a^m, we sample a chunk of actions a^c of length l_c from Gaussian distribution, where the i-th action is represented as $a_i^c \sim \mathcal{N}(a^m, \sigma)$. This ensures consistent exploration and avoids the zero-mean random action issue that confines the agent to a small vicinity near the start state.

Recent works have also employed action chunking (Bharadhwaj et al., 2024b; Zhao et al., 2023) in behavior cloning. However, our application is different and we propose to use action chunking to enable more effective unsupervised exploration. We illustrate how, in combination with video-guided exploration, this action chunking allows for more coherent exploration, as well as enabling models to make consistent plans to achieve video goals. In Section 4.3, we provide a study comparing chunk-level prediction versus single action prediction in the Libero environment and empirically show that the chunk-level design can substantially improve the resulting goal-reaching policy.

4 Experiments

We present our experiment results across four simulated environments shown in Figure 2. In Section 4.1, we describe our results on three robotic manipulation environments: 8 tasks on Libero (Liu et al., 2024), 6 tasks on MetaWorld (Yu et al., 2020), and 4 tasks on Calvin (Mees et al., 2022). Following this, in Section 4.2, we show evaluation results on 4 different scenes and 12 targets on iTHOR (Kolve et al., 2017) visual navigation environment. Finally, in Section 4.3, we present ablation studies on the proposed chunk level action prediction and random action bootstrapping methods. We provide more experiment results in Appendix A and B. We use the same demonstration data to train the baseline methods and our video model, *except that* training the video model only requires the image sequences of demonstrations, while most baseline methods need the corresponding action annotations (highlighted by an asterisk). In evaluation, for manipulation tasks, the initial robot state and object positions are randomized; for visual navigation tasks, we randomize the robot start position.

Implementation. For the video model, the inputs are the observation image and the task description. We follow the lightweight video model architecture introduced in (Ko et al., 2023) and train one video model from scratch for each environment. We deem that finetuning large text-conditioned video models (Yang et al., 2024e; Chen et al., 2024; Saharia et al., 2022) or designing task-specific

	put-red-mug-left	put-red-mug-right	put-white-mug-left	put-Y/W-mug-right	Overall
BC*	8.8±5.3	15.2±7.8	32.0±12.9	21.6±12.3	19.4±9.6
GCBC*	2.4±2.0	0.8±1.6	16.0±7.2	7.2±5.3	6.6±4.0
DP BC*	33.6±3.2	33.6±8.2	59.2±7.8	57.6±5.4	46.0±6.2
DP GCBC*	24.8±4.7	22.4±7.4	16.0±8.8	3.2±3.0	16.6±6.0
SuSIE*	18.4±2.0	32.0±8.4	43.2±4.7	25.6±11.5	29.8±6.6
AVDC	0.0±0.0	0.0±0.0	0.0±0.0	0.0±0.0	0.0±0.0
Ours w/ SuSIE	23.2±3.0	**60.0**±6.7	**68.8**±4.7	**67.2**±8.9	**54.8**±5.8
Ours	**38.4**±15.3	40.8±7.8	51.2±3.9	38.4±8.6	42.2±8.9

	put-choc-left	put-choc-right	put-red-mug-plate	put-white-mug-plate	Overall
BC*	19.2±9.3	12.8±9.3	7.2±5.3	20.0±11.3	14.8±8.8
GCBC*	4.8±1.6	4.0±4.4	2.4±3.2	7.2±6.4	4.6±3.9
DP BC*	42.4±5.4	50.4±5.4	32.8±9.3	71.2±5.3	49.2±6.4
DP GCBC*	45.6±6.0	32.0±8.8	7.2±4.7	5.6±4.1	22.6±5.9
SuSIE*	17.6±9.3	32.8±9.9	16.0±2.5	10.4±4.1	19.2±6.5
AVDC	1.3±1.9	0.0±0.0	0.0±0.0	0.0±0.0	0.3±0.5
Ours w/ SuSIE	44.0±7.6	54.4±5.4	66.4±12.0	**36.0**±7.6	50.2±8.2
Ours	**70.4**±12.8	**79.2**±3.9	**72.8**±6.4	25.6±11.5	**62.0**±8.7

Table 1: **Quantitative results on 8 tasks of two different scenes in Libero.** Note that methods marked with an asterisk '*' require ground-truth action demonstrations to train, while other methods do not. *Ours w/ SuSIE* uses an image-editing model to generate subgoals guidance while *Ours* uses a video model.

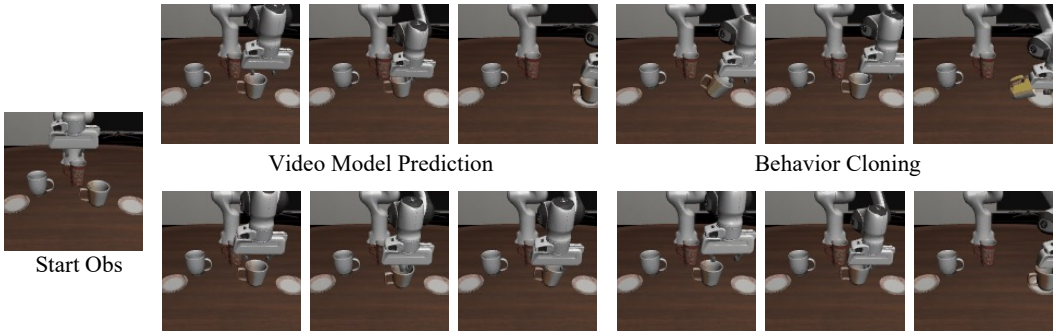

Figure 3: **Qualitative Results of task 'put the yellow and white mug to the right plate' in Libero environment.** The start states of the robot and objects are randomized in test-time. Only a subset of the predicted video frames are shown due to space limit. Our goal-conditioned policy shown in the bottom left is able to follow the video prediction and finish the task. BC cannot accurately locate the target while AVDC can move to the mug but without the skill of grasping concave objects.

video model might be an interesting future research direction. For the goal-conditioned policy, we implement it with a CNN-based Diffusion Policy (Chi et al., 2023), which takes as input the observation image and the goal image and outputs a chunk of actions. For detailed implementation of our method and each baseline, please refer to Appendix D.

4.1 Manipulation

In this section, we aim to evaluate the goal-conditioned policy learned by the proposed unsupervised exploration in tabletop manipulation environments with continuous action space. To better understand the capability of the method, we investigate multi-task policy learning in Libero and Calvin, and single-task policy learning in Meta-world. Note that methods highlighted by an *asterisk* require ground-truth action labels to train, whereas our method only requires image demonstration sequences to train the video model and self-supervised training for the policy model.

Libero (Liu et al., 2024) is a tabletop simulation of a Franka Robot, which features several dexterous manipulation tasks. For each task in Libero, the agent is required to achieve the final state described in a corresponding sentence, which identifies the target object and task completion state. The action space consists of the delta position and orientation of the end effector and the applied force on the gripper, resulting in a total dimension of 7.

	door-open	door-close	handle-press	hammer	assembly	faucet-open	Overall
BC*	64.0±4.4	76.0±0.0	49.6±3.2	4.8±3.9	8.0±2.5	88.8±3.0	48.5±2.8
GCBC*	64.8±6.9	93.6±2.0	50.4±6.5	4.8±1.6	8.0±2.5	**95.2**±1.6	52.8±3.5
DP BC*	73.6±4.8	94.4±2.0	52.0±8.4	7.2±3.0	0.8±1.6	82.4±2.0	51.7±3.6
DP GCBC*	68.0±0.0	96.0±4.0	36.0±0.0	14.0±2.0	5.6±2.0	80.0±0.0	49.9±1.3
AVDC	52.0±0.0	**97.3**±1.9	76.0±5.7	4.0±3.3	8.0±0.0	66.7±5.0	50.7±2.6
Ours	**76.0**±4.9	85.6±2.0	**94.4**±2.0	**43.2**±6.4	**16.8**±3.0	**87.2**±3.0	67.2±3.6

Table 2: **Quantitative Results of 6 tasks in Meta-World.** Methods marked with an asterisk '*' require ground-truth action demonstrations to train. AVDC uses the segmentation mask of the target object to compute actions. Our method learns the policy by video-guided self-exploration in the environment without any external supervision.

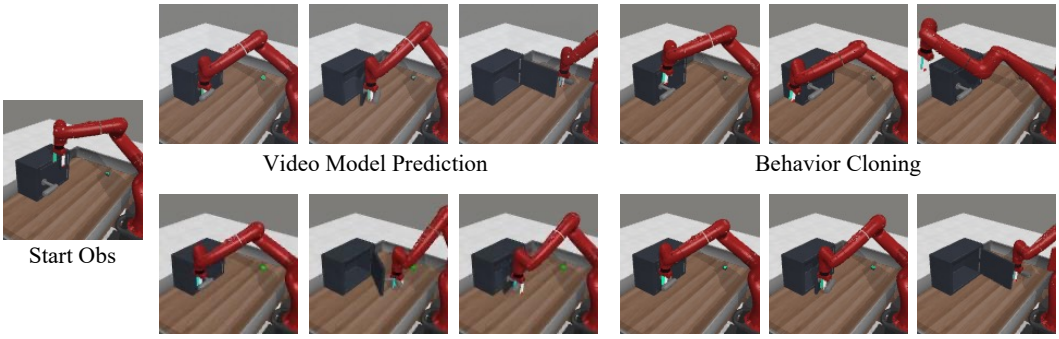

Figure 4: **Qualitative Results of task Door-Open in Meta-World environment.** The position of the box and robot are randomized in test-time. Only a subset of the predicted video frames are shown due to space limit. Our goal-conditioned policy can follow the subgoals given by the video frames and successfully finish the task. BC misses the handle probably due to the out of training distribution box position and starts to predict random actions. AVDC can move to the handle thanks to the exact given handle location. However, it begins to close the door halfway, probably because of the incorrect flow prediction due to error accumulation or occlusion.

We include 8 tasks from two scenes in Libero as the testbed. In this environment, we aim to evaluate multi-task learning capability of our method, hence we only train one policy model for all 8 tasks. The video model is trained on the visual image sequences of the demonstrations provided in Libero, where we use 20 episodes per task, thereby 160 demonstrations in total. We train BC, GCBC, SuSIE (Black et al., 2023) on the same visual image sequences but with expert actions corresponding to each image. Following the setting in AVDC, we provide it with the segmentation masks of the target objects, while our method does not require such privilege information.

We present the quantitative results in Table 1 and qualitative results in Figure 3 and 6. Across 8 tasks, our method is able to outperform the baselines by a margin, though without any access to expert action data. We observe that BC-based methods tend to memorize and overfit to the training data, where they fails to locate the target objects, while our method is more robust in test-time. In addition, though knowing the exact positions of target objects in test-time, AVDC is unable to achieve any meaningful results, probably because that AVDC uses hard-coded action primitives and planning procedural, making it difficult to generalize to more complex manipulation task, for example, grasping concave objects such as mugs. Note that our method can also be integrated with various forms of generative models, as shown by *Ours w/ SuSIE* where we use an image-editing model to predict the subgoals for exploration. Please refer to Appendix A for more results and Appendix C for failure analysis.

Meta-World (Yu et al., 2020) is a simulated robotic benchmark of a Sawyer robot arm with a set of tabletop manipulation tasks that involve various object interactions and different tool use. The action space consists of the delta position of the end effector and the applied force on the gripper, resulting in a total dimension of 4.

We consider 6 tasks: door-open, door-close, handle-press, hammer, assembly, faucet-open. We directly utilize the video model checkpoint provided in AVDC. To further validate the proposed exploration approach, we conduct single-task exploration in this environment, where we train one policy model for each task. Each learning-based baseline model is trained on the same demonstrations used to train the video model, namely, 15 episodes per task. We present the quantitative results in Table 2 and qualitative results in Figure 4. We observe that our policies can successfully learn

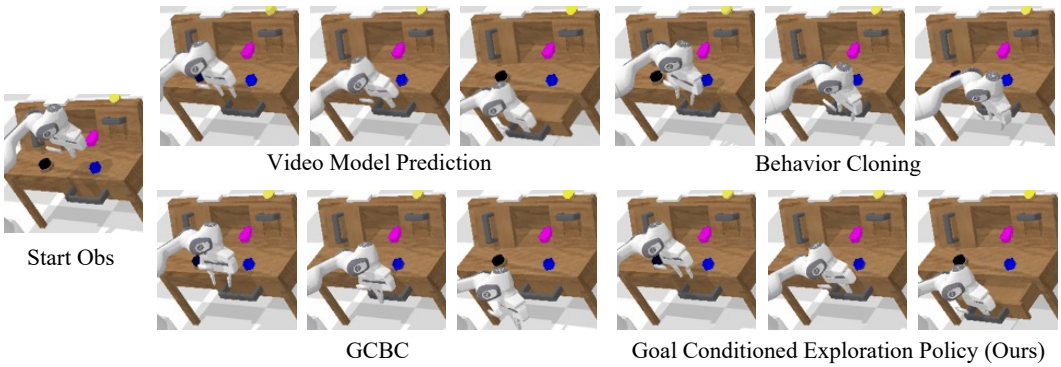

Figure 5: **Qualitative Results of task Open Drawer in Calvin environment.** Our goal conditioned policy successfully completes the task by following the subgoals in the video, while both BC and GCBC cannot put the end effector to the handle and thus fail to open the drawer.

	lightbulb	led	slider left	open drawer	Overall
BC*	47.2±21.1	48.8±9.9	67.2±14.2	36.0±18.8	49.8±16.0
GCBC*	1.6±2.0	38.4±13.0	32.0±6.2	22.4±7.8	23.6±7.3
DP BC*	70.4±2.0	79.2±3.9	68.8±4.7	56.8±1.6	68.8±3.0
DP GCBC*	35.2±3.0	44.0±5.7	40.0±3.6	17.6±7.4	34.2±4.9
Ours	**100.0**±0.0	**86.4**±5.4	**83.2**±3.0	**68.0**±3.6	**84.4**±3.0

Table 3: **Quantitative Results of 4 Calvin tasks**. Each task requires the agent to manipulate objects located in different regions, especially in open drawer where the policy need to cover the bottom right boundary of the environment.

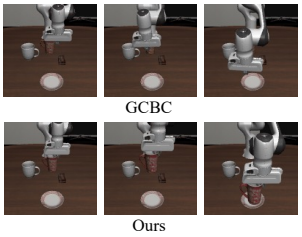

Figure 6: **Qualitative Comparison of our method and GCBC on Libero.**

various manipulation skills and outperform all the counterparts in the average success rate despite the absence of action labels for training. In addition, we also compare with training a single-task RL with a zero-shot reward function in Appendix A.7.

Calvin (Mees et al., 2022) is a robotic simulation environment with multiple language-conditioned tasks. This environment contains a 7-DOF Panda robot arm and various assets including a desk with a sliding door, a drawer, an LED, and a lightbulb. The agent is required to complete tasks in the environment given by a corresponding language description. The action space we use is same as Libero.

We consider 4 tasks: turn on lightbulb, turn on led, move slider left, and open drawer. These tasks involve different manipulation skills and different operation areas in the workspace, allowing us to validate skill learning and spatial coverage capability of our goal-conditioned policy. For example, to move slider left, the agent has to drag the handle from the central area to the upper left corner. We present the quantitative results in Table 3 and qualitative results in Figure 5. We do not report AVDC in the above table, as we found it performed very poorly in the above environments. Even without any action data or rewards, our policy is able to cover the majority of the space and outperform all the baselines, especially for the challenging open drawer task, where the agent must move downwards below the table and pull toward the bottom right boundary of the environment.

4.2 Visual Navigation

In addition to tabletop-level robot arm manipulation tasks, we evaluate the proposed method in a room-level visual navigation setting with discrete actions.

iTHOR (Kolve et al., 2017) is a room-level vision-based simulated environment, where agents can navigate in the scenes and interact with objects. We adopt the iTHOR visual object navigation benchmark, where agents are required to navigate to the specific type of objects given by a natural language input. The action space consists of four actions: Move Ahead, Turn Left, Turn Right, and Done. We incorporate 4 different scene types: Kitchen, Living Room, Bedroom, and Bathroom, with 3 targets in each scene. Following (Ko et al., 2023), the video model is trained on 20 demonstration image sequences per task. BC and GCBC are also trained on the same demonstrations while with access to corresponding actions. Since the navigation actions are discrete and episode lengths (typically < 20) are much shorter than robot arm manipulation tasks, we find that predicting a single action suffices. Our method uses the same ResNet+MLP model architecture as BC-based baselines.

Figure 7: **Qualitative Results of Navigation to Bread in iTHOR environment.** The start position of the agent is randomized in test-time. Only a subset of the predicted video frames are shown due to space limit. In navigation task with a moving camera, the video model can still generate realistic frames that respect the the actual scene layout. Our goal-conditioned policy is able to follow the video frames and reach the bread shown in the middle of the frame. However, BC turns to the other way, and AVDC cannot correctly infer the required actions and miss the target.

	Kitchen				Living Room			
Method	Toaster	Spatula	Bread	Overall	Painting	Laptop	Television	Overall
BC*	48.0±2.4	56.0±3.7	**36.0**±6.6	46.7±4.3	**36.0**±12.4	45.0±11.0	49.0±4.9	43.3±9.4
GCBC*	**52.0**±5.1	49.0±6.6	39.0±5.8	46.7±5.9	27.0±8.1	**49.0**±5.8	**58.0**±8.7	**44.7**±7.6
AVDC	10.0±4.1	13.3±4.7	13.3±2.4	12.2±3.7	8.3±2.4	13.3±8.5	20.0±4.1	13.9±5.0
Ours	45.0±3.2	**56.0**±4.9	**44.0**±5.8	**48.3**±4.6	29.0±4.9	42.0±6.0	**57.0**±5.1	**42.7**±5.3

	Bedroom				Bathroom			
Method	Blinds	DeskLamp	Pillow	Overall	Mirror	ToiletPaper	SoapBar	Overall
BC*	**67.0**±2.4	**40.0**±7.1	**81.0**±5.8	**62.7**±5.1	**48.0**±6.8	51.0±13.2	45.0±4.5	48.0±8.1
GCBC*	52.0±8.1	22.0±2.4	72.0±6.0	48.7±5.5	43.0±16.0	64.0±9.2	55.0±11.8	54.0±12.3
AVDC	30.0±4.1	13.3±4.7	36.7±2.4	26.7±3.7	10.0±4.1	1.7±2.4	6.7±2.4	6.1±2.9
Ours	**57.0**±5.1	24.0±3.7	**72.0**±7.5	**51.0**±5.4	36.0±9.2	**75.0**±4.5	**47.0**±7.5	**52.7**±7.0

Table 4: **Quantitative Results on iThor Navigation.** We report the success rates across 4 different scenes and 12 targets. Though without access to action labels, our method is on par with the BC and GCBC trained on expert demonstrations and outperforms AVDC which also does not require expert action labels.

We present the quantitative results in Table 4. Our method outperforms the no expert data baseline AVDC by 36% on average and surpasses all baselines in the Kitchen scene while performing on par with BC-based baselines in other scenes. Qualitative results are shown in Figure 7 and 15. Our goal-conditioned policy is able to reliably synthesize discrete actions that follow the generated video plan. In contrast, the actions inferred by AVDC are incorrect: the agent keeps rotating right and misses the target, whereas the underlying actions in the video should be moving ahead and then rotating right, probably because that the drastic change in observation poses challenges for optical flow prediction. BC predicts a wrong action at the first step, where the agent directly rotates to the opposite side and navigates to the target Spatula, likely due to its limited generalizability – directly mimicking the similar actions in the training demonstrations at this position.

4.3 Ablation Studies

In this section, we ablate the effectiveness of design choices described in Section 3. We provide additional studies in Appendix A, including training with different amounts of data, video exploration frequency q_v, and different horizons of the video model and goal-conditioned policy.

Random Action Bootstrapping. We conduct ablation studies on the importance of the random action bootstrapping technique. We first present the training-time exploration efficiency in Figure 8. As shown by *w/o rand*, the no random action method tends to collapse and can hardly achieve any task success during the exploration. Since the task completion data cannot be collected from the environment, *w/o rand* cannot obtain any meaningful results in test-time, which is reflected in Table 5. In contrast, as shown by the blue, red, and orange lines in Figure 8, the model is able to obtain significantly more task success after we apply random action bootstrapping. The performance of *w/o extra rand* decreases through time in Scene 1, showing that extra random exploration is able to

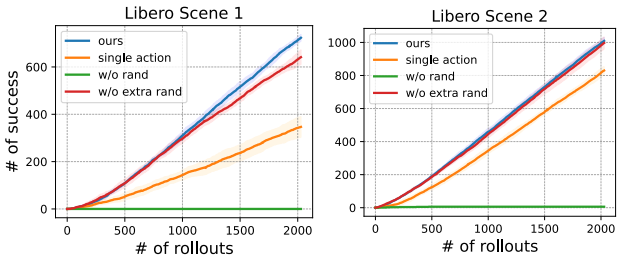

Figure 8: **Line Chart of Number of Success versus Number of Total Exploration Rollouts During Training.** Both *ours*, *w/o extra rand*, *single action* can effectively complete tasks during exploration and are also consistent to their test-time performance.

Method	Scene 1	Scene 2
w/o rand	0.0±0.0	0.0±0.0
w/o video	0.0±0.0	0.0±0.0
w/o extra rand	28.0±5.0	61.6±9.6
single action	16.4±5.4	41.0±5.8
Ours	**42.2**±8.9	**62.0**±8.7

Table 5: **Ablation Studies on Exploration in Libero environment.** We report experiment results of w/o any random bootstrapping, w/o video-guided exploration, w/ initial but w/o extra random bootstrapping, using a single action prediction model along with our proposed approach.

stabilize training, and its performance is similar to *ours* in Scene 2, probably because the manipulation region for Scene 2 focuses on the center area of the table (see Figure 11) and the initial random actions suffice. Besides, we observe that the slope of the curve gradually become stable after just 250 rollout attempts, which means that the success rate of exploration can easily converge, showing the efficiency of the proposed video-guided exploration scheme.

Chunk-level Action Prediction. We compare the performance of the proposed chunk-level action prediction model v.s. single action prediction model. We use the same setup as BC (ResNet18+MLP) for the *single action* prediction baseline. We first present a line chart of the number of success during exploration v.s. total number of exploration rollouts in Figure 8. Both the chunk-level method and the single action method achieve non-trivial numbers of success during exploration. However, we can see that the chunk-level model consistently obtains higher success rates (i.e., steeper slope) in the exploration phase, which facilitates the policy learning because the training data contains more trajectories that successfully complete the tasks. In Table 5, we present the test-time success rate of the two methods in Libero. Similar to the exploration phase, the chunk-level action prediction model achieves higher success rates by 25.8% and 21.0%, respectively.

Video Guided Environment Exploration. We further compare the performance of purely random action exploration versus with video-guided exploration, as shown by *w/o video* in Table 5, where we replace the video-guided exploration in Algorithm 1 by random exploration. Unsurprisingly, the purely random exploration baseline fails across all tasks. We hypothesize that without guidance from the video model, the agent can hardly discover the necessary states to complete the tasks, probably due to the long temporal distance between the start and goal states and the fact that the relevant state space for task completion only accounts for a tiny subset of the infinite possible states.

5 Discussion

Limitations. Our approach has several limitations. First, since the approach relies on goal-conditioned random exploration and without access to action labels, for tasks that require very precise manipulation (*i.e.* stacking a block tower in millimeter precision), our random exploration procedure may not find the precise set of actions. In such settings, having a random exploration primitive (i.e. stacking a block on top of another) on which we do goal-conditioned policy learning may help us find such precise actions. In addition, purely random exploration in the physical world might pose additional requirements for the workbench, as sampled actions or the initial actions outputted by the learned goal-conditioned policy may cause undesired contacts between the robot and the external environment. This can be partially mitigated by integrating hard-coded safety constraints and is also a further direction of future work. Moreover, our method might demand more training computation compared to direct behavior cloning from expert demonstrations, due to the cost of video model and additional training iterations. Finally, our method usually requires dozens of video-guided rollouts to obtain a competent policy for a task. While resetting an environment is easy in simulation, this might demand additional work in real-world experiments. Combining our approach with a policy that can reset environment states would be an interesting direction for future.

Conclusion. In this paper, we have presented a self-supervised approach to ground generated videos into actions. As generative video models become increasingly more powerful, we believe that they will be increasingly useful for decision-making, providing powerful priors on how various tasks should be accomplished. As a result, the question of how we can accurately convert generated video plans to actual physical execution will become increasingly more relevant, and our approach points towards one direction to solve this question, through online interaction with the agent's environment.

BIBLIOGRAPHY

Anurag Ajay, Seungwook Han, Yilun Du, Shuang Li, Abhi Gupta, Tommi Jaakkola, Josh Tenenbaum, Leslie Kaelbling, Akash Srivastava, and Pulkit Agrawal. Compositional foundation models for hierarchical planning. *Advances in Neural Information Processing Systems*, 36, 2024. 2

Bowen Baker, Ilge Akkaya, Peter Zhokov, Joost Huizinga, Jie Tang, Adrien Ecoffet, Brandon Houghton, Raul Sampedro, and Jeff Clune. Video pretraining (vpt): Learning to act by watching unlabeled online videos. *Advances in Neural Information Processing Systems*, 35:24639–24654, 2022. 2

Marc Bellemare, Sriram Srinivasan, Georg Ostrovski, Tom Schaul, David Saxton, and Remi Munos. Unifying count-based exploration and intrinsic motivation. *Advances in neural information processing systems*, 29, 2016. 3

Homanga Bharadhwaj, Roozbeh Mottaghi, Abhinav Gupta, and Shubham Tulsiani. Track2act: Predicting point tracks from internet videos enables diverse zero-shot robot manipulation. *arXiv preprint arXiv:2405.01527*, 2024a. 2

Homanga Bharadhwaj, Jay Vakil, Mohit Sharma, Abhinav Gupta, Shubham Tulsiani, and Vikash Kumar. Roboagent: Generalization and efficiency in robot manipulation via semantic augmentations and action chunking. In *2024 IEEE International Conference on Robotics and Automation (ICRA)*, pp. 4788–4795. IEEE, 2024b. 5

Kevin Black, Mitsuhiko Nakamoto, Pranav Atreya, Homer Walke, Chelsea Finn, Aviral Kumar, and Sergey Levine. Zero-shot robotic manipulation with pretrained image-editing diffusion models. *arXiv preprint arXiv:2310.10639*, 2023. 1, 2, 7

Tim Brooks, Bill Peebles, Connor Holmes, Will DePue, Yufei Guo, Li Jing, David Schnurr, Joe Taylor, Troy Luhman, Eric Luhman, Clarence Ng, Ricky Wang, and Aditya Ramesh. Video generation models as world simulators. In *OpenAI*, 2024. URL https://openai.com/research/video-generation-models-as-world-simulators. 1, 2

Jake Bruce, Michael Dennis, Ashley Edwards, Jack Parker-Holder, Yuge Shi, Edward Hughes, Matthew Lai, Aditi Mavalankar, Richie Steigerwald, Chris Apps, et al. Genie: Generative interactive environments. *arXiv preprint arXiv:2402.15391*, 2024. 2

Annie S Chen, Suraj Nair, and Chelsea Finn. Learning generalizable robotic reward functions from" in-the-wild" human videos. *arXiv preprint arXiv:2103.16817*, 2021. 2

Haoxin Chen, Yong Zhang, Xiaodong Cun, Menghan Xia, Xintao Wang, Chao Weng, and Ying Shan. Videocrafter2: Overcoming data limitations for high-quality video diffusion models. In *Proceedings of the IEEE/CVF Conference on Computer Vision and Pattern Recognition*, pp. 7310–7320, 2024. 5

Cheng Chi, Siyuan Feng, Yilun Du, Zhenjia Xu, Eric Cousineau, Benjamin Burchfiel, and Shuran Song. Diffusion policy: Visuomotor policy learning via action diffusion. *arXiv preprint arXiv:2303.04137*, 2023. 6, 18, 29, 31

Yilun Du, Sherry Yang, Pete Florence, Fei Xia, Ayzaan Wahid, Pierre Sermanet, Tianhe Yu, Pieter Abbeel, Joshua B Tenenbaum, Leslie Pack Kaelbling, et al. Video language planning. In *The Twelfth International Conference on Learning Representations*, 2023. 1

Yilun Du, Sherry Yang, Bo Dai, Hanjun Dai, Ofir Nachum, Josh Tenenbaum, Dale Schuurmans, and Pieter Abbeel. Learning universal policies via text-guided video generation. *Advances in Neural Information Processing Systems*, 36, 2024. 1, 2

Alejandro Escontrela, Ademi Adeniji, Wilson Yan, Ajay Jain, Xue Bin Peng, Ken Goldberg, Youngwoon Lee, Danijar Hafner, and Pieter Abbeel. Video prediction models as rewards for reinforcement learning. *Advances in Neural Information Processing Systems*, 36, 2024. 2

Benjamin Eysenbach, Abhishek Gupta, Julian Ibarz, and Sergey Levine. Diversity is all you need: Learning skills without a reward function. In *International Conference on Learning Representations*, 2019. 3

Dibya Ghosh, Abhishek Gupta, Ashwin Reddy, Justin Fu, Coline Manon Devin, Benjamin Eysenbach, and Sergey Levine. Learning to reach goals via iterated supervised learning. In *International Conference on Learning Representations*, 2021. 3

Rohit Girdhar, Mannat Singh, Andrew Brown, Quentin Duval, Samaneh Azadi, Sai Saketh Rambhatla, Akbar Shah, Xi Yin, Devi Parikh, and Ishan Misra. Emu video: Factorizing text-to-video generation by explicit image conditioning. *arXiv preprint arXiv:2311.10709*, 2023. 1

Tuomas Haarnoja, Aurick Zhou, Pieter Abbeel, and Sergey Levine. Soft actor-critic: Off-policy maximum entropy deep reinforcement learning with a stochastic actor. In *International conference on machine learning*, pp. 1861–1870. PMLR, 2018. 3

Danijar Hafner, Timothy Lillicrap, Jimmy Ba, and Mohammad Norouzi. Dream to control: Learning behaviors by latent imagination. *arXiv preprint arXiv:1912.01603*, 2019. 3

Kaiming He, Xiangyu Zhang, Shaoqing Ren, and Jian Sun. Deep residual learning for image recognition. In *Proceedings of the IEEE conference on computer vision and pattern recognition*, pp. 770–778, 2016. 31

Mikael Henaff. Explicit explore-exploit algorithms in continuous state spaces. *Advances in Neural Information Processing Systems*, 32, 2019. 3

Jonathan Ho, William Chan, Chitwan Saharia, Jay Whang, Ruiqi Gao, Alexey Gritsenko, Diederik P Kingma, Ben Poole, Mohammad Norouzi, David J Fleet, et al. Imagen video: High definition video generation with diffusion models. *arXiv preprint arXiv:2210.02303*, 2022. 1

Edward S Hu, Richard Chang, Oleh Rybkin, and Dinesh Jayaraman. Planning goals for exploration. In *The Eleventh International Conference on Learning Representations*, 2022. 3

Tao Huang, Guangqi Jiang, Yanjie Ze, and Huazhe Xu. Diffusion reward: Learning rewards via conditional video diffusion. *arXiv preprint arXiv:2312.14134*, 2023. 2

Arnav Kumar Jain, Lucas Lehnert, Irina Rish, and Glen Berseth. Maximum state entropy exploration using predecessor and successor representations. In *Thirty-seventh Conference on Neural Information Processing Systems*, 2023. 3

Ziwei Ji, Nayeon Lee, Rita Frieske, Tiezheng Yu, Dan Su, Yan Xu, Etsuko Ishii, Ye Jin Bang, Andrea Madotto, and Pascale Fung. Survey of hallucination in natural language generation. *ACM Computing Surveys*, 55(12):1–38, 2023. 27

Po-Chen Ko, Jiayuan Mao, Yilun Du, Shao-Hua Sun, and Joshua B Tenenbaum. Learning to act from actionless videos through dense correspondences. In *The Twelfth International Conference on Learning Representations*, 2023. 1, 2, 5, 8, 17, 20, 29, 31

Eric Kolve, Roozbeh Mottaghi, Winson Han, Eli VanderBilt, Luca Weihs, Alvaro Herrasti, Matt Deitke, Kiana Ehsani, Daniel Gordon, Yuke Zhu, et al. Ai2-thor: An interactive 3d environment for visual ai. *arXiv preprint arXiv:1712.05474*, 2017. 5, 8

Ilya Kostrikov, Denis Yarats, and Rob Fergus. Image augmentation is all you need: Regularizing deep reinforcement learning from pixels. *arXiv preprint arXiv:2004.13649*, 2020. 19

Qiyang Li, Jason Zhang, Dibya Ghosh, Amy Zhang, and Sergey Levine. Accelerating exploration with unlabeled prior data. *Advances in Neural Information Processing Systems*, 36, 2024. 2

Junbang Liang, Ruoshi Liu, Ege Ozguroglu, Sruthi Sudhakar, Achal Dave, Pavel Tokmakov, Shuran Song, and Carl Vondrick. Dreamitate: Real-world visuomotor policy learning via video generation. *arXiv preprint arXiv:2406.16862*, 2024. 2

Zhan Ling, Yunchao Yao, Xuanlin Li, and Hao Su. On the efficacy of 3d point cloud reinforcement learning. *arXiv preprint arXiv:2306.06799*, 2023. 29

Bo Liu, Yifeng Zhu, Chongkai Gao, Yihao Feng, Qiang Liu, Yuke Zhu, and Peter Stone. Libero: Benchmarking knowledge transfer for lifelong robot learning. *Advances in Neural Information Processing Systems*, 36, 2024. 5, 6

Yecheng Jason Ma, Shagun Sodhani, Dinesh Jayaraman, Osbert Bastani, Vikash Kumar, and Amy Zhang. Vip: Towards universal visual reward and representation via value-implicit pre-training. *arXiv preprint arXiv:2210.00030*, 2022. 2

Yecheng Jason Ma, Vikash Kumar, Amy Zhang, Osbert Bastani, and Dinesh Jayaraman. Liv: Language-image representations and rewards for robotic control. In *International Conference on Machine Learning*, pp. 23301–23320. PMLR, 2023. 2, 19

Robert McCarthy, Daniel CH Tan, Dominik Schmidt, Fernando Acero, Nathan Herr, Yilun Du, Thomas G Thuruthel, and Zhibin Li. Towards generalist robot learning from internet video: A survey. *arXiv preprint arXiv:2404.19664*, 2024. 2

Oier Mees, Lukas Hermann, Erick Rosete-Beas, and Wolfram Burgard. Calvin: A benchmark for language-conditioned policy learning for long-horizon robot manipulation tasks. *IEEE Robotics and Automation Letters*, 7(3):7327–7334, 2022. 5, 8

Russell Mendonca, Shikhar Bahl, and Deepak Pathak. Structured world models from human videos. *arXiv preprint arXiv:2308.10901*, 2023. 2

Deepak Pathak, Pulkit Agrawal, Alexei A Efros, and Trevor Darrell. Curiosity-driven exploration by self-supervised prediction. In *International conference on machine learning*, pp. 2778–2787. PMLR, 2017. 3

Silviu Pitis, Harris Chan, Stephen Zhao, Bradly Stadie, and Jimmy Ba. Maximum entropy gain exploration for long horizon multi-goal reinforcement learning. In *International Conference on Machine Learning*, pp. 7750–7761. PMLR, 2020. 3

Vitchyr H Pong, Murtaza Dalal, Steven Lin, Ashvin Nair, Shikhar Bahl, and Sergey Levine. Skew-fit: state-covering self-supervised reinforcement learning. In *Proceedings of the 37th International Conference on Machine Learning*, pp. 7783–7792, 2020. 3

Ilija Radosavovic, Xiaolong Wang, Lerrel Pinto, and Jitendra Malik. State-only imitation learning for dexterous manipulation. In *2021 IEEE/RSJ International Conference on Intelligent Robots and Systems (IROS)*, pp. 7865–7871. IEEE, 2021. 2

Oleh Rybkin, Karl Pertsch, Konstantinos G Derpanis, Kostas Daniilidis, and Andrew Jaegle. Learning what you can do before doing anything. *arXiv preprint arXiv:1806.09655*, 2018. 2

Chitwan Saharia, William Chan, Saurabh Saxena, Lala Li, Jay Whang, Emily L Denton, Kamyar Ghasemipour, Raphael Gontijo Lopes, Burcu Karagol Ayan, Tim Salimans, et al. Photorealistic text-to-image diffusion models with deep language understanding. *Advances in neural information processing systems*, 35:36479–36494, 2022. 5

Cansu Sancaktar, Sebastian Blaes, and Georg Martius. Curious exploration via structured world models yields zero-shot object manipulation. *Advances in Neural Information Processing Systems*, 35:24170–24183, 2022. 3

Karl Schmeckpeper, Oleh Rybkin, Kostas Daniilidis, Sergey Levine, and Chelsea Finn. Reinforcement learning with videos: Combining offline observations with interaction. In *Conference on Robot Learning*, pp. 339–354. PMLR, 2021. 2

Ramanan Sekar, Oleh Rybkin, Kostas Daniilidis, Pieter Abbeel, Danijar Hafner, and Deepak Pathak. Planning to explore via self-supervised world models. In *International conference on machine learning*, pp. 8583–8592. PMLR, 2020. 3

Younggyo Seo, Kimin Lee, Stephen L James, and Pieter Abbeel. Reinforcement learning with action-free pre-training from videos. In *International Conference on Machine Learning*, pp. 19561–19579. PMLR, 2022. 2

Pranav Shyam, Wojciech Jaśkowski, and Faustino Gomez. Model-based active exploration. In *International conference on machine learning*, pp. 5779–5788. PMLR, 2019. 3

Richard S Sutton. Reinforcement learning: An introduction. *A Bradford Book*, 2018. 4

Faraz Torabi, Garrett Warnell, and Peter Stone. Behavioral cloning from observation. In *Proceedings of the 27th International Joint Conference on Artificial Intelligence*, pp. 4950–4957, 2018. 2

Boyang Wang, Nikhil Sridhar, Chao Feng, Mark Van der Merwe, Adam Fishman, Nima Fazeli, and Jeong Joon Park. This&that: Language-gesture controlled video generation for robot planning. *arXiv preprint arXiv:2407.05530*, 2024. 2

Jianren Wang, Sudeep Dasari, Mohan Kumar Srirama, Shubham Tulsiani, and Abhinav Gupta. Manipulate by seeing: Creating manipulation controllers from pre-trained representations. In *Proceedings of the IEEE/CVF International Conference on Computer Vision*, pp. 3859–3868, 2023. 2

Chuan Wen, Xingyu Lin, John So, Kai Chen, Qi Dou, Yang Gao, and Pieter Abbeel. Any-point trajectory modeling for policy learning. *arXiv preprint arXiv:2401.00025*, 2023. 2

Hongtao Wu, Ya Jing, Chilam Cheang, Guangzeng Chen, Jiafeng Xu, Xinghang Li, Minghuan Liu, Hang Li, and Tao Kong. Unleashing large-scale video generative pre-training for visual robot manipulation. *arXiv preprint arXiv:2312.13139*, 2023. 2

Jialong Wu, Haoyu Ma, Chaoyi Deng, and Mingsheng Long. Pre-training contextualized world models with in-the-wild videos for reinforcement learning. *Advances in Neural Information Processing Systems*, 36, 2024. 2

Dongjie Yang, Suyuan Huang, Chengqiang Lu, Xiaodong Han, Haoxin Zhang, Yan Gao, Yao Hu, and Hai Zhao. Vript: A video is worth thousands of words. *arXiv preprint arXiv:2406.06040*, 2024a. 27

Jiange Yang, Bei Liu, Jianlong Fu, Bocheng Pan, Gangshan Wu, and Limin Wang. Spatiotemporal predictive pre-training for robotic motor control. *arXiv preprint arXiv:2403.05304*, 2024b. 2

Sherry Yang, Yilun Du, Seyed Kamyar Seyed Ghasemipour, Jonathan Tompson, Leslie Pack Kaelbling, Dale Schuurmans, and Pieter Abbeel. Learning interactive real-world simulators. In *The Twelfth International Conference on Learning Representations*, 2024c. 1, 2

Sherry Yang, Jacob Walker, Jack Parker-Holder, Yilun Du, Jake Bruce, Andre Barreto, Pieter Abbeel, and Dale Schuurmans. Video as the new language for real-world decision making. *arXiv preprint arXiv:2402.17139*, 2024d. 2

Zhuoyi Yang, Jiayan Teng, Wendi Zheng, Ming Ding, Shiyu Huang, Jiazheng Xu, Yuanming Yang, Wenyi Hong, Xiaohan Zhang, Guanyu Feng, et al. Cogvideox: Text-to-video diffusion models with an expert transformer. *arXiv preprint arXiv:2408.06072*, 2024e. 5

Denis Yarats, Rob Fergus, Alessandro Lazaric, and Lerrel Pinto. Mastering visual continuous control: Improved data-augmented reinforcement learning. *arXiv preprint arXiv:2107.09645*, 2021. 19

Tianhe Yu, Deirdre Quillen, Zhanpeng He, Ryan Julian, Karol Hausman, Chelsea Finn, and Sergey Levine. Meta-world: A benchmark and evaluation for multi-task and meta reinforcement learning. In *Conference on robot learning*, pp. 1094–1100. PMLR, 2020. 5, 7

Yanjie Ze, Gu Zhang, Kangning Zhang, Chenyuan Hu, Muhan Wang, and Huazhe Xu. 3d diffusion policy. *arXiv preprint arXiv:2403.03954*, 2024. 29

Tony Z Zhao, Vikash Kumar, Sergey Levine, and Chelsea Finn. Learning fine-grained bimanual manipulation with low-cost hardware. *arXiv preprint arXiv:2304.13705*, 2023. 5

Enshen Zhou, Yiran Qin, Zhenfei Yin, Yuzhou Huang, Ruimao Zhang, Lu Sheng, Yu Qiao, and Jing Shao. Minedreamer: Learning to follow instructions via chain-of-imagination for simulated-world control. *arXiv preprint arXiv:2403.12037*, 2024a. 2

Siyuan Zhou, Yilun Du, Jiaben Chen, Yandong Li, Dit-Yan Yeung, and Chuang Gan. Robodreamer: Learning compositional world models for robot imagination. *arXiv preprint arXiv:2404.12377*, 2024b. 2

APPENDIX

Table of Contents

A Additional Quantitative Results

In this section, we provide additional quantitative experiment results. In Section A.1, we compare our methods with BC trained on more demonstration data. Next, in Section A.2, we investigate the effect of training the video model with different amounts of demonstration data. In Section A.3, we experiment our proposed method with video models of different horizons. In Section A.4, we study the exploration performance with different video exploration frequency q_v. Following this, in Section A.5, we conduct experiments on different horizons of the goal-conditioned policy we use in exploration.

A.1 BC with More Data

We provide comparison of our policy learned by unsupervised exploration and plain BC with increasing amount of training data. To train these BC baselines, We use the official demonstrations provided by Libero. For example, BC 10 means that we use 10 demonstrations per task to train the BC model (resulting in 80 demonstrations in total). The reported results are average across 5 checkpoints. Note that our policy does not need any action labels and directly learn how to ground the goals given by the video model via exploration in the environment. The video model is trained with 20 demonstrations, which only requires images. That said, this is not a completely fair comparison, but we include this comparison to better illustrate the difficulty of the tasks.

We report the results in Table 6. The success rate of our method even outperforms BC trained with 50 demonstrations per task, while our policy is learned purely by exploration, which indicates that efficacy of the proposed exploration method. We also observe that though the success rate of BC generally increases over more training data, BC 20 is able to slightly outperform BC 30 in Scene 1 while BC 30 slightly outperforms BC 40 in Scene 2. Since the BC model is trained on 8 tasks, the heterogeneous task structures can result in fluctuation in the success rate (the model might bias towards some specific tasks).

	put-red-mug-left	put-red-mug-right	put-white-mug-left	put-Y/W-mug-right	Overall
BC 10	2.4±3.2	8.8±6.9	23.2±12.0	5.6±4.1	10.0±6.5
BC 20	8.8±5.3	15.2±7.8	32.0±12.9	21.6±12.3	19.4±9.6
BC 30	9.6±4.1	14.4±9.0	28.0±9.1	15.2±11.1	16.8±8.3
BC 40	8.0±5.1	11.2±5.3	44.8±19.8	21.6±12.0	21.4±10.6
BC 50	12.8±8.9	20.0±12.9	40.0±12.1	18.4±6.0	22.8±10.0
Ours	**38.4**±15.3	**40.8**±7.8	**51.2**±3.9	**38.4**±8.6	**42.2**±8.9

	put-choc-left	put-choc-right	put-red-mug-plate	put-white-mug-plate	Overall
BC 10	3.2±3.0	4.0±5.1	2.4±4.8	6.4±4.1	4.0±4.2
BC 20	19.2±9.3	12.8±9.3	7.2±5.3	20.0±11.3	14.8±8.8
BC 30	13.6±12.0	31.2±15.9	5.6±6.0	16.8±10.6	16.8±11.1
BC 40	13.6±5.4	28.0±10.4	7.2±6.4	12.8±5.3	15.4±6.9
BC 50	19.2±9.3	24.0±10.4	12.8±7.8	24.8±4.7	20.2±8.0
Ours	**70.4**±12.8	**79.2**±3.9	**72.8**±6.4	**25.6**±11.5	**62.0**±8.7

Table 6: **BC with Different Amount of Data in Libero Environment.**

A.2 Video Model with Different Amounts of Data

We investigate the effects of training the video model with different amounts of demonstration data. For the result shown in Table 1 in the main paper, we use 20 demonstrations per task to train the video model. In this section, we provide two ablation studies that use 10 demonstrations per task and 50 demonstrations per task, as shown in Table 7 below.

The performance of our method increases in both scenes as with more training data. While the performance uniformly increases in Scene 1, we observe that in some specific tasks of Scene 2, the performance slightly decreases. This might be due to the learning capacity of the underlying goal reaching policy, since we only train one policy model for all eight tasks. In general, we believe that by scaling up the data size, data diversity, and model complexity can further buttress the performance.

	put-red-mug-left	put-red-mug-right	put-white-mug-left	put-Y/W-mug-right	Overall
train size 10	18.4±8.2	31.2±4.7	22.4±2.0	44.8±5.9	29.2±5.2
train size 20	38.4±15.3	40.8±7.8	51.2±3.9	38.4±8.6	42.2±8.9
train size 50	**40.0**±10.7	**54.4**±9.0	**69.6**±14.9	**57.6**±9.7	**55.4**±11.1

	put-choc-left	put-choc-right	put-red-mug-plate	put-white-mug-plate	Overall
train size 10	68.0±6.7	78.4±4.1	63.2±6.4	19.2±5.3	57.2±5.6
train size 20	**70.4**±12.8	79.2±3.9	**72.8**±6.4	25.6±11.5	62.0±8.7
train size 50	67.2±5.9	**84.8**±6.4	67.2±6.9	**52.0**±11.3	**67.8**±7.6

Table 7: **Training the Video Model with Different Amount of Data.**

A.3 Video Model with Different Horizons

We study the effect of different video model horizons in this section. We follow the training procedure of the video model in (Ko et al., 2023): during training, given a start image observation, we uniformly sample h images between the start image and the final task completion image and use these h images as supervision signals. That said, a longer video horizon h will generate a denser subgoal sequence. Following (Ko et al., 2023), we set horizon $h = 7$ across all our experiments except for this ablation study in Table 8.

As shown in Table 8, our method is able to maintain a similar performance across different video horizons. We observe that performance decreases when video horizon is set to 9. One potential reason is that the modeling complexity increases when we increase the prediction horizon, while we keep the same video model architecture, suggesting that we should learn video models over a sparser set of video frames.

	put-red-mug-left	put-red-mug-right	put-white-mug-left	put-Y/W-mug-right	Overall
Video Horizon 7	38.4±15.3 %	40.8±7.8 %	51.2±3.9 %	38.4±8.6 %	42.2±8.9 %
Video Horizon 8	28.8±3.0 %	59.2±5.3 %	52.0±8.8 %	54.4±9.3 %	48.6±6.6 %
Video Horizon 9	17.6±5.4 %	65.6±9.7 %	38.4±8.6 %	30.4±3.2 %	38.0±6.7 %

	put-choc-left	put-choc-right	put-red-mug-plate	put-white-mug-plate	Overall
Video Horizon 7	70.4±12.8 %	79.2±3.9 %	72.8±6.4 %	25.6±11.5 %	62.0±8.7 %
Video Horizon 8	46.4±6.5 %	69.6±10.9 %	64.0±4.4 %	31.2±8.5 %	52.8±7.6 %
Video Horizon 9	52.0±6.7 %	70.4±3.2 %	68.8±6.9 %	13.6±7.8 %	51.2±6.2 %

Table 8: **Video Model with Different Horizons.**

A.4 Different Video Exploration Frequency

In this section, we study the effect of video exploration frequency. For example, when q_v is set to 200, we conduct one video-guided exploration for each task every 200 training iterations. The trade-off between smaller and larger q_v is that: if q_v is small, the agent will conduct exploration in a higher frequency, where the replay buffer will refresh faster and contain more latest rollout data. If q_v is large, the agent conducts exploration less frequently, which might enable the agent to better fit and digest the existing data in the replay buffer. We provide ablation studies on 5 different q_v on Libero environment, as shown in Figure 9.

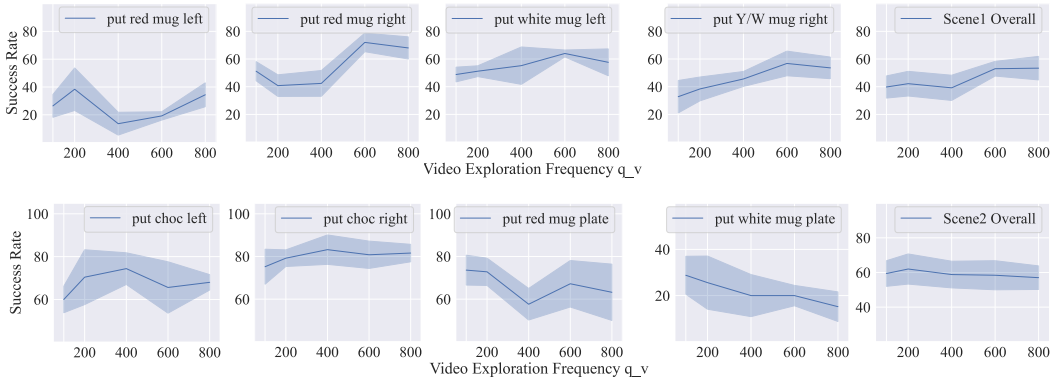

Figure 9: **Different Video Exploration Frequency q_v.** $q_v = 200$ indicates that we conduct one video-guided exploration for each task every 200 training iterations. Thus, the agent will conduct with more exploration with lower q_v while less exploration with higher q_v. Our method performs steadily across different values of q_v.

Figure 9 shows that our method perform steadily across various q_v, ranging from 100 to 800. Note that when q_v is set to 800, the video exploration is four times smaller than our default setting ($q_v = 200$), which means that our method can achieve a comparable performance with much fewer environment interactions.

A.5 Different Policy Horizon for our Goal Conditioned Policy

In this section, we study the effect of using different horizons for the diffusion policy based goal-conditioned policy. We set the policy horizons to 12, 16, 20, 24 with the same CNN-based architecture. We observe that the policy learned by the proposed exploration pipeline is robust to the different horizons value, and obtain the highest success rate when horizon = 16, which also conforms to the reported results in Diffusion Policy (Chi et al., 2023). Please refer to Table 9 for quantitative results.

	put-red-mug-left	put-red-mug-right	put-white-mug-left	put-Y/W-mug-right	Overall
Horizon=12	21.6±7.4 %	**56.8**±4.7 %	43.2±9.9 %	47.2±6.9 %	**42.2**±7.2 %
Horizon=16	**38.4**±15.3 %	40.8±7.8 %	**51.2**±3.9 %	38.4±8.6 %	**42.2**±8.9 %
Horizon=20	13.6±6.0 %	50.4±7.8 %	48.0±7.2 %	37.6±7.0 %	37.4±7.0 %
Horizon=24	21.6±6.0 %	36.8±4.7 %	40.8±8.5 %	**48.8**±8.5 %	37.0±6.9 %

	put-choc-left	put-choc-right	put-red-mug-plate	put-white-mug-plate	Overall
Horizon=12	62.4±10.3 %	**80.0**±7.2 %	56.0±7.2 %	**25.6**±8.6 %	56.0±8.3 %
Horizon=16	**70.4**±12.8 %	79.2±3.9 %	**72.8**±6.4 %	**25.6**±11.5 %	**62.0**±8.7 %
Horizon=20	64.8±14.2 %	76.0±5.1 %	68.8±15.3 %	18.4±6.0 %	57.0±10.1 %
Horizon=24	60.0±12.1 %	68.8±10.6 %	37.6±13.8 %	20.8±7.3 %	46.8±10.9 %

Table 9: **Different Horizons for the Goal Conditioned Policy.**

A.6 Different Training Timesteps

In this section, we investigate the model performance at different training timesteps on Libero environment, specifically, when the model is trained for $40k$, $80k$, $120k$, $160k$, and $200k$ steps. We set the video exploration frequency q_v to 200 in this experiment. We observe that the overall success rate of the two scenes stabilize after $80k$ training steps. However, the per-task success rate oscillates through further training. This might be caused by the recent collected data in the replay buffer (which is used for training) and the task level interference.

	put-red-mug-left	put-red-mug-right	put-white-mug-left	put-Y/W-mug-right	Overall
$40k$	34.4±7.4	37.6±12.0	28.8±4.7	32.0±10.4	33.2±8.6
$80k$	**63.2**±9.3	**72.0**±6.7	48.8±6.9	**42.4**±4.1	**56.6**±6.7
$120k$	47.2±8.5	56.0±4.4	**58.4**±9.3	38.4±4.8	50.0±6.8
$160k$	33.6±7.4	43.2±5.9	53.6±6.5	33.6±10.9	41.0±7.7
$200k$	38.4±15.3	40.8±7.8	51.2±3.9	38.4±8.6	42.2±8.9

	put-choc-left	put-choc-right	put-red-mug-plate	put-white-mug-plate	Overall
$40k$	13.6±9.0	14.4±6.0	9.6±6.0	5.6±2.0	10.8±5.7
$80k$	47.2±6.9	58.4±8.6	68.8±6.9	15.2±5.9	47.4±7.1
$120k$	51.2±3.0	70.4±8.6	68.0±6.7	23.2±8.2	53.2±6.6
$160k$	66.4±8.6	74.4±5.4	**75.2**±5.3	16.0±8.0	58.0±6.8
$200k$	**70.4**±12.8	**79.2**±3.9	72.8±6.4	**25.6**±11.5	**62.0**±8.7

Table 10: **Performance at Different Training Steps in Libero Environment.**

A.7 Comparison to RL with Zero-Shot Reward

In this section, we compare our method to a reinforcement learning baseline. Since our method do not have access to environment rewards, we leverage a foundational zero-shot robotic model to generate the rewards. Specifically, we adopt DrQ (Kostrikov et al., 2020; Yarats et al., 2021) and LIV (Ma et al., 2023) as the RL method and foundation model respectively. We use the potential based reward defined in LIV.

We present the results in Table 11. We see that DrQ+LIV fails to make meaningful progress in five out of six tasks, achieving only an 8% success rate in the handle-press task. We observe that one probable cause is that the generated reward signals are ambiguous, which hinders the RL method to learn. For instance, it is challenging for the model to generate a significant positive reward upon task completion and the rewards may oscillate even when positive progress is being made.

	door-open	door-close	handle-press	hammer	assembly	faucet-open	Overall
DrQ + LIV	0.0±0.0	0.0±0.0	8.0±0.0	0.0±0.0	0.0±0.0	0.0±0.0	1.3±0.0
Ours	**76.0**±4.9	85.6±2.0	**94.4**±2.0	**43.2**±6.4	**16.8**±3.0	**87.2**±3.0	67.2±3.6

Table 11: **Quantitative Comparison to DrQ+LIV on 6 tasks from Meta-World.**

A.8 Policy Robustness to Video Models of Different Sampling Rates

In this section, we study the robustness of the resulting goal-conditioned policy learned by exploration to the video models of different sampling rates. Specifically, once the policy is trained, we replace the training-time video model with video models of different sampling rates while remain using the same policy.

Following the video model design in Ko et al. (2023), we use the *Number of Frames to Goal* to denote the sampling rate of the video model. For example, *Number of Frames to Goal = 9* indicates that the video model is designed to uniformly generate 9 frames from the initial observation to the goal state, that is, compared to a 7-frame video model, the sampling rate is denser (i.e., the temporal distance between two adjacent frames is smaller).

We present the policy success rate in Table 12. In this table, the policy is trained with a 7-frame video model (marked with an asterisk) while the number of frames to goal of the test-time video model varies from 5 to 9. The policy consistently achieves high performance across video models with different sampling rates, demonstrating its robustness to variations in the sampling rate during testing. This is probably because of the robust policy training enabled by the combination of random action bootstrapping and video-guided exploration.

We observe that the 6-frame video model attains the highest success rate, even surpassing the training-time 7-frame model. This improvement is likely due to the better quality of the synthesized video frames, as modeling a greater or denser number of frames increases complexity while we keep the video model size unchanged in this experiment.

# Frames to Goal	put-red-mug-left	put-red-mug-right	put-white-mug-left	put-Y/W-mug-right	Overall
5	32.8±12.0	46.4±10.3	66.4±5.4	**41.6**±4.8	46.8±8.1
6	38.4±4.8	48.0±8.8	**68.8**±4.7	36.0±6.7	**47.8**±6.2
7*	38.4±15.3	40.8±7.8	51.2±3.9	38.4±8.6	42.2±8.9
8	**39.2**±6.4	**51.2**±13.7	65.6±4.8	25.6±5.4	45.4±7.6
9	32.8±5.3	44.0±8.8	36.8±9.9	28.8±5.9	35.6±7.5

# Frames to Goal	put-choc-left	put-choc-right	put-red-mug-plate	put-white-mug-plate	Overall
5	62.4±4.1	76.8±11.7	66.4±4.1	**59.2**±10.6	66.2±7.6
6	64.8±6.9	72.0±12.4	**74.4**±9.3	58.4±9.3	**67.4**±9.5
7*	**70.4**±12.8	79.2±3.9	72.8±6.4	25.6±11.5	62.0±8.7
8	52.0±12.1	**84.8**±8.2	68.0±8.4	26.4±10.9	57.8±9.9
9	59.2±13.9	76.0±8.8	**74.4**±9.7	20.8±7.3	57.6±9.9

Table 12: **Policy Performance with Video Models of Different Sampling Rates at Test Time.** All results in the table are from the same goal-conditioned policy but with video models of different sampling rates (identified by the number of intermediate frames from initial observation to the goal state). The policy uses a video model of *# Frames to Goal = 7* to conduct video-guided exploration during training, but is evaluated with video models of different numbers of to-goal frames at test time. The policy performs consistently and is robust to various sampling rates at test time.

B Additional Qualitative Results

In this section, we present additional qualitative results in both tabletop manipulation environment and visual navigation environment. For extra results and side-by-side qualitative comparison on our, please refer to our website.

B.1 Libero

In this section, we provide additional qualitative results of our method on 8 tasks in Libero environment, as shown in Figure 10 and 11. For each episode, we show the generated video in the first row and the rollout results of our goal conditioned policy learned by self-supervised exploration in the second row.

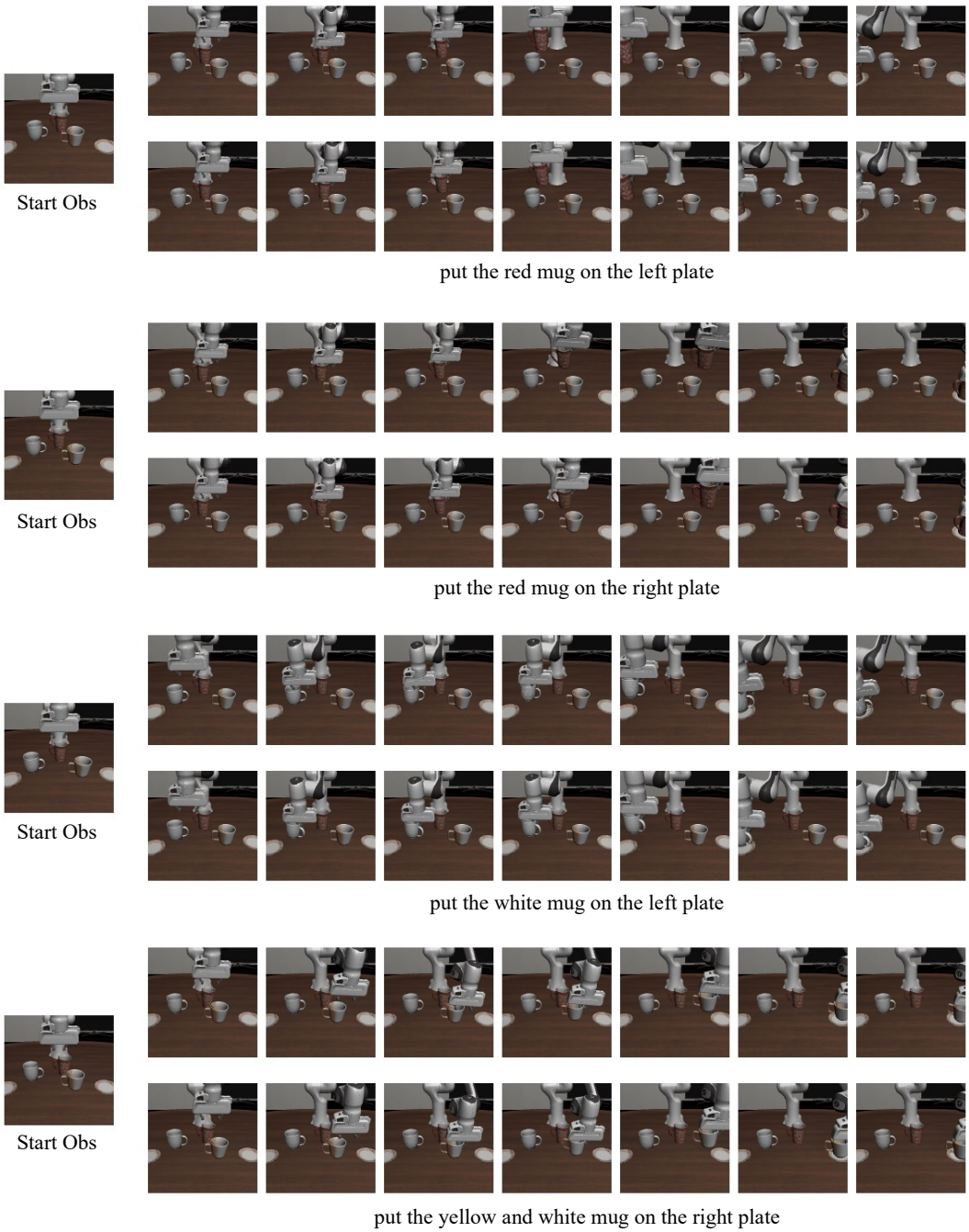

Figure 10: **Additional Qualitative Results of the Generated Videos and Our Policy Rollout on Libero Scene 1.** We present qualitative results of four tasks in Libero Scene 1. For each task, results are displayed in 2 rows: the first row of images are the generated video from the video model conditioned on the start observation image and task description, and the second row of images are the rollout of our policy conditioned on the corresponding frames from the generated video. The task description provided to the video model are shown below the respective images.

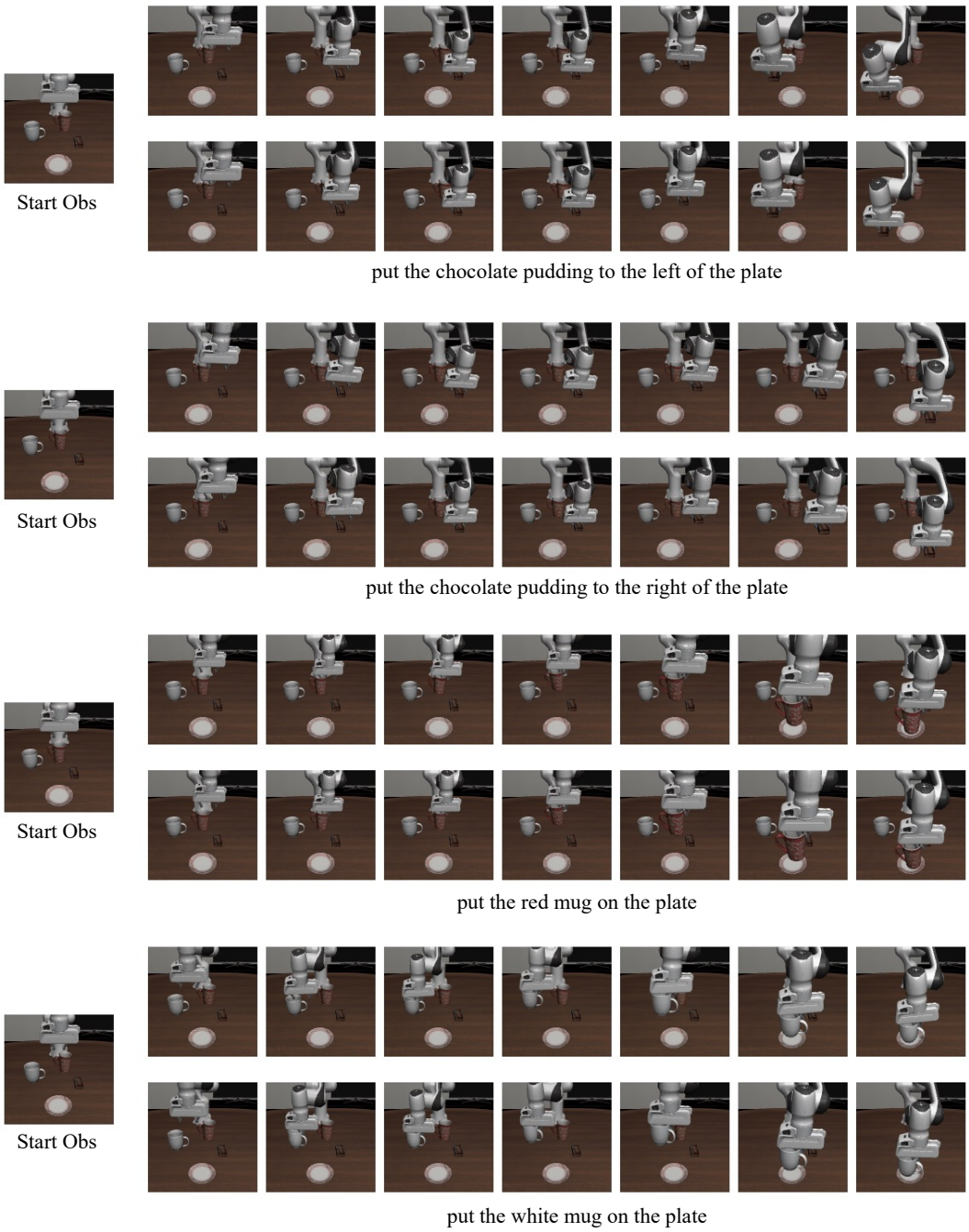

Figure 11: **Additional Qualitative Results of the Generated Videos and Our Policy Rollout on Libero Scene 2.** We present qualitative results of four tasks in Libero Scene 2. For each task, results are displayed in 2 rows: the first row of images are the generated video from the video model conditioned on the start observation image and task description, and the second row of images are the rollout of our policy conditioned on the corresponding frames from the generated video. The task description provided to the video model are shown below the respective images.

B.2 META-WOLRD

In this section, we provide additional qualitative results of our method on 6 tasks in Meta-World environment, as shown in Figure 12 and 13. For each episode, we show the generated video in the

first row, and the rollout results of our goal conditioned policy learned by self-supervised exploration in the second row.

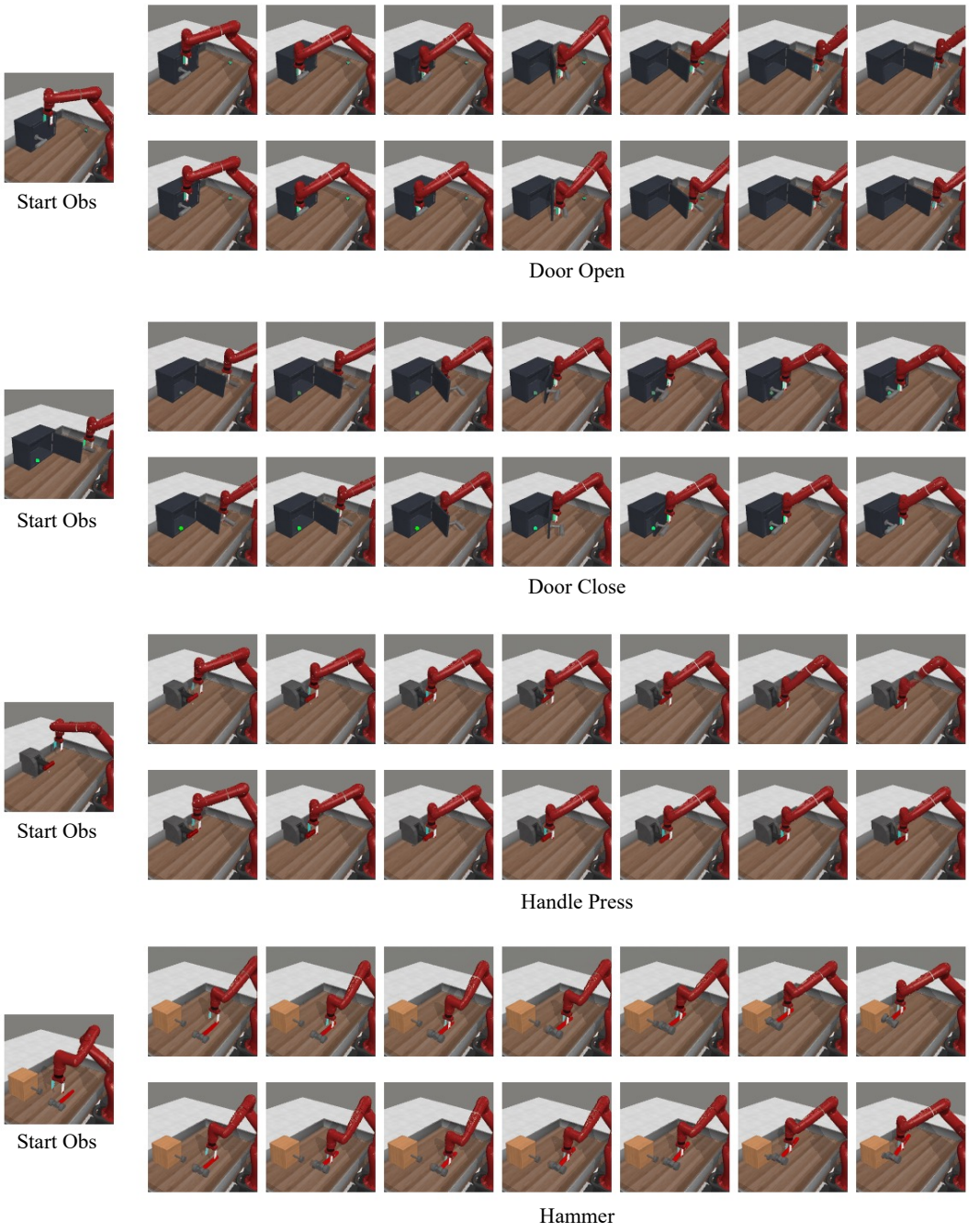

Figure 12: **Additional Qualitative Results of the Generated Videos and Our Policy Rollout of 4 tasks on Meta-World.** We present qualitative results of four tasks in Meta-World Environment. For each task, results are displayed in 2 rows: the first row of images are the generated video from the video model conditioned on the start observation image and task description, and the second row of images are the rollout of our policy conditioned on the corresponding frames from the generated video. The task prompts provided to the video model are shown below the respective images.

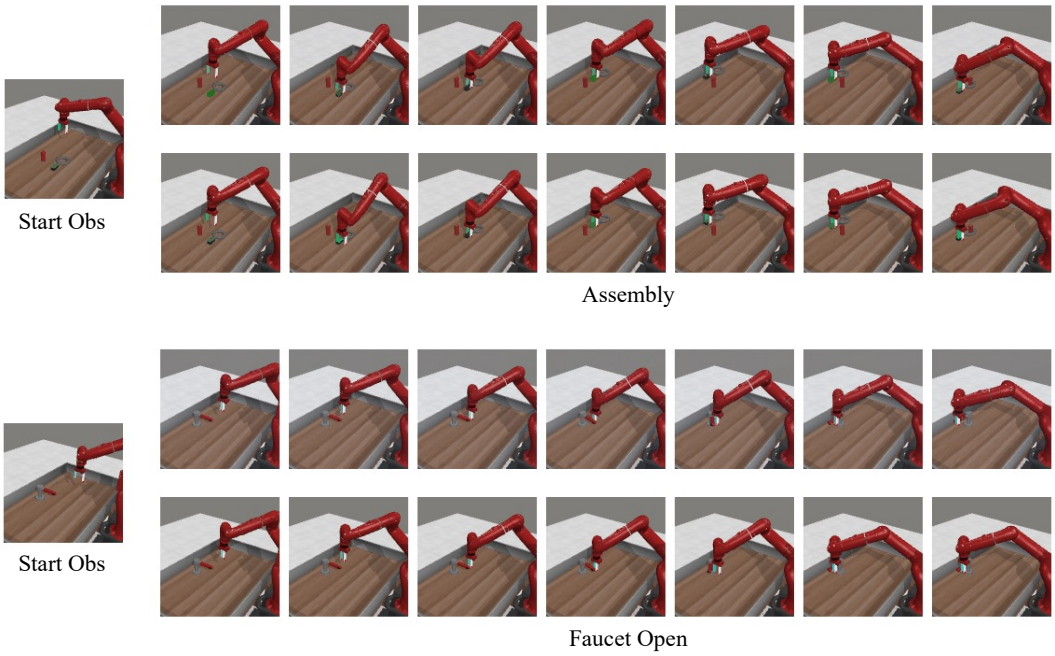

Figure 13: **Additional Qualitative Results of the Generated Videos and Our Policy Rollout of 2 tasks on Meta-World.** We present qualitative results of four tasks in Meta-World Environment. For each task, results are displayed in 2 rows: the first row of images are the generated video from the video model conditioned on the start observation image and task description, and the second row of images are the rollout of our policy conditioned on the corresponding frames from the generated video. The task prompt provided to the video model are shown below the respective images.

B.3 CALVIN

In this section, we provide additional qualitative results of our method on 4 tasks in Calvin environment, as shown in Figure 14. For each episode, we show the generated video in the first row, and the rollout results of our goal conditioned policy learned by self-supervised exploration in the second row.

Figure 14: **Additional Qualitative Results of the Generated Videos and Our Policy Rollout of 4 tasks on Calvin.** We present qualitative results of four tasks in Calvin Environment. For each task, results are displayed in 2 rows: the first row of images are the generated video from the video model conditioned on the start observation image and task description, and the second row of images are the rollout of our policy conditioned on the corresponding frames from the generated video. The task prompt provided to the video model are shown below the respective images.

B.4 iTHOR VISUAL NAVIGATION

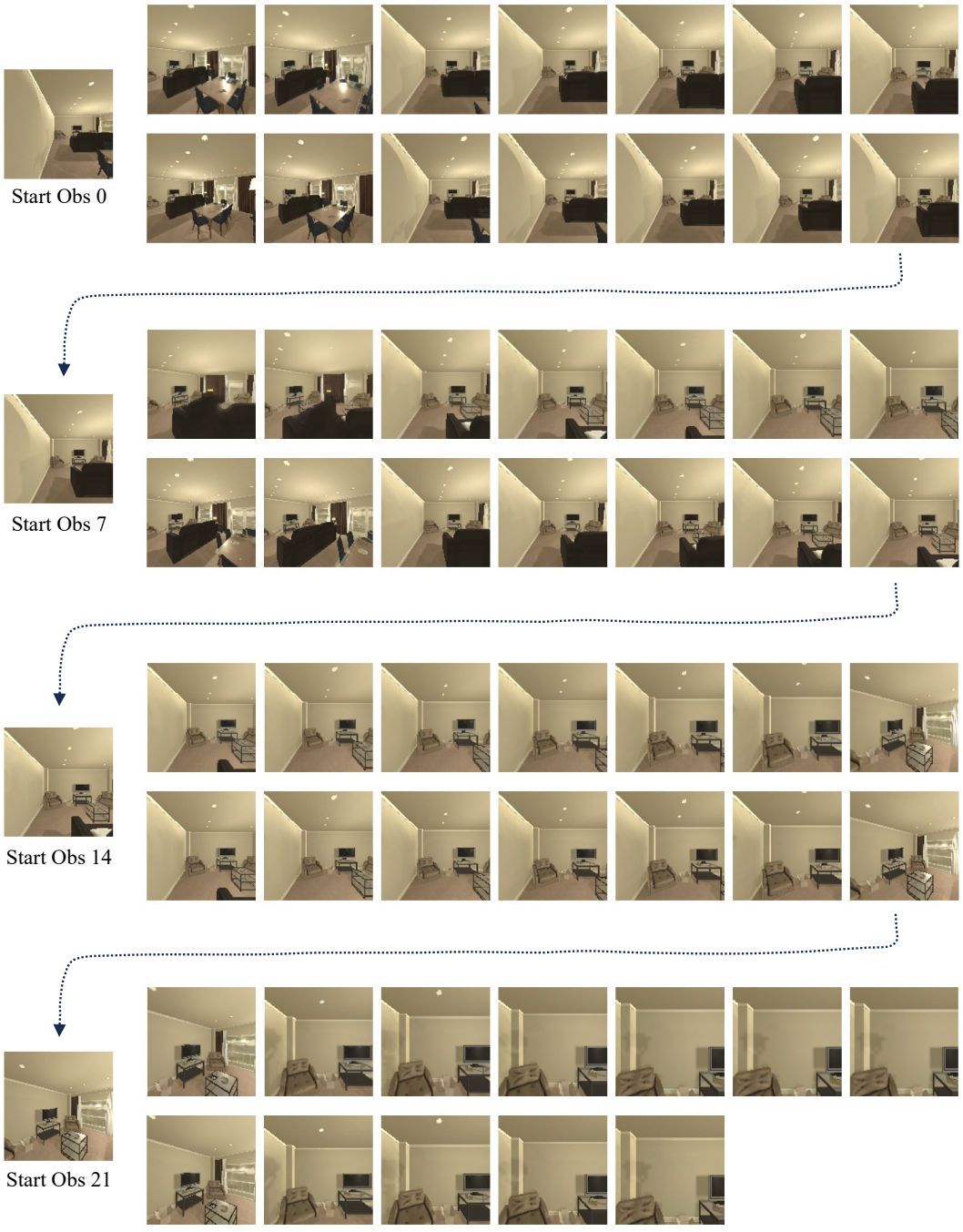

Figure 15: **Four Consecutive Policy Rollout for one Evaluation Episode in a Living Room Scene of iTHOR.** In each rollout, the first row of images are the generated video from the video model conditioned on the start observation image (shown in the leftmost column) and task description (name of the target). The second row of images are the rollout of our policy conditioned on the corresponding frames from the generated video. The names of the scene and target are shown at the bottom. Due to the long spatial distance, the agent takes more than 20 actions to navigate to the television, which corresponds to the four videos above. The last observation of the previous rollout is fed to the video model to generate future subgoals, as indicated by the dashed arrows.

In this section, we provide additional qualitative results of the generated videos and our goal conditioned policy learned by self-supervised exploration in a Living Room Scene (FloorPlan201) of iTHOR visual navigation environments, as shown in Figure 15. Starting at *Start Obs 0*, the agent is tasked to navigate to the television at the other end of the room, which typically requires more than 20 actions to reach. While the horizon of the video model is only 7, we consecutively generate future subgoals by feeding the last observation image to the video model as condition (indicated by the dashed arrows). With four video predictions and 26 actions, the agent successfully navigates to the television, showing the long and consecutive rollout capability of our policy.

C Failure Mode Analysis

In the previous section, we demonstrate that our method is able to achieve non-trivial performance in various robotic environments. However, the method still poses some limitations, which lead to failure. In this section, we provide analysis into the failure mode of our method. We categorize the causes to video model based and policy learning based.

C.1 Video Model

The performance of the video model is one influential factor of the success rate because that if an incorrect subgoal is given, even though the policy is accurate enough, the task cannot be completed.

Hallucination is a common issue for generative models (Yang et al., 2024a; Ji et al., 2023). We also observe some extent of hallucination in our video model. We present some visualizations in Figure 16.

In Table 1, *Ours* and *Ours w/ SuSIE* only achieve 25.6% and 36.0% on the task 'put the white mug on the plate'. We observe that one major cause of this relatively low performance is the heavy hallucination in the generated video of this task, as shown in the first row of Figure 16. We hypothesize that this might partially due to the dataset imbalance problem, as we have two tasks involving chocolate pudding while only one for white mug in this scene, considering that only 20 demonstrations are provided for each task.

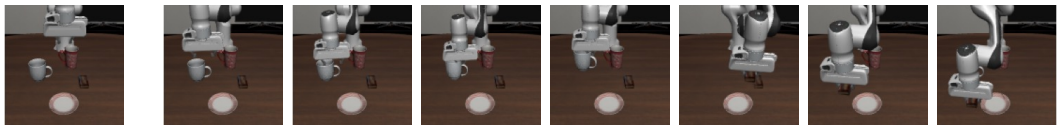

Start Obs — Hallucination in Video Model of 'put the white mug on the plate'

Start Obs — Hallucination in Video Model of 'put the yellow and white mug on the right plate'

Figure 16: **Failure Mode: Video Model Hallucination.** In the first row, the given prompt to the video model is 'put the white mug on the plate'. Though the first four frames generated by the video model are on the right path for achieving the goal, the white mug is suddenly replaced by the chocolate pudding in the following frames, which will subsequently confuse the policy. In the second row, the given prompt to the video model is 'put the yellow and white mug on the right plate'. Similarly, the agent in the video frames first correctly approaches the yellow and white mug, but the yellow and white mug is replaced by a red mug in the intermediate frames.

Mismatch of Task and Generated Videos Given a specific task description, we observe that the video model might generate a video that is actually for completing another task. For example, given the task description of 'put the chocolate pudding to the *left* of the plate', the video model might generate a video that 'put the chocolate pudding to the *right* of the plate'. One potential cause is the relatively close embedding distance between these two sentences as well as the corresponding videos, making the model generate a similar but incorrect video. We provide some visualizations in Figure 17.

We believe that these issue can be mitigated by multiple ways, such as improving the video model architecture, scaling up the training data, finetuning from existing pre-trained large video model, or using the environment interaction feedback to correct the video model, which might be interesting future research directions.

Start Obs — Mismatch Video Prediction of 'put the white mug on the left plate'

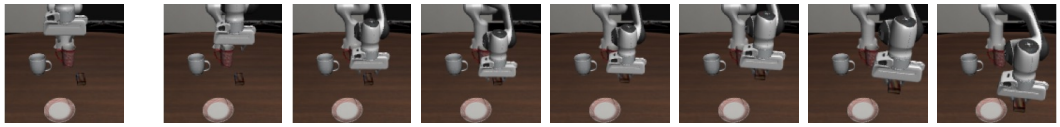

Start Obs — Mismatch Video Prediction of 'put the chocolate pudding to the left of the plate'

Figure 17: **Failure Mode: Mismatch of the Task and the Generated Video.** In the first row, the given prompt to the video model is 'put the white mug on the left plate', while the generated video puts the red cup to the left plate. In the second row, the given prompt to the video model is 'put the chocolate pudding to the left of the plate', while the generated video puts the chocolate pudding to the right of the plate.

Video Model Prediction

Policy Failure: Mug Displacement

Figure 18: **Failure Mode: Precision, Libero.** A failure case of 'put the red mug on the left plate' in Libero Scene 1. We only show the results of the last three subgoals. Though the goal conditioned policy is able to successfully put the red mug on the left plate in the last frame, a slight displacement is introduced (see the rightmost column), which results in task failure.

Video Model Prediction

Policy Failure: Nut Touches the Peg

Figure 19: **Failure Mode: Precision, Meta-World.** A failure case of the assembly task. We only show the results of the last three subgoals. In this episode, the goal conditioned policy exactly follows the subgoals in the first two frames, but in the last frame (the rightmost column), the nut touches the peg due to slight precision error and hence fails to insert the nut into to peg, resulting in task failure.

C.2 Policy Learning

Policy learning is particularly challenging in our unsupervised setting, since we assume no action demonstrations nor rewards. Generally, we observe that the learned policy is able to follow the video model, but there remain challenges for the policy to handle fine-grained tasks that require precise control. For example, our policy achieves 94.4% at handle press task, while only achieves 16.8% at assembly task in Meta-World. In Figure 18 and Figure 19, we provide some qualitative results of failure cases in Libero and Meta-World.

In Figure 18, we present a failure case of the task 'put the red mug on the left plate' in Libero. In this task, the agent needs to put the red mug at the center of the left plate within a small tolerance. One major reason of the policy's failure is that the mug is not precisely placed at the center, as shown in the rightmost column.

In Figure 19, we present a failure case of the task assembly in Meta-World. In this task, the agent needs to pick up a nut and precisely place it onto a peg. While the policy seems to exactly follow the given subgoals, it fails to insert the nut at the last frame where the nut undesirably touches the peg.

One potential way to increase the performance is to design some replanning strategies. Another interesting direction to improve the policy is to better leverage the geometric information. Currently, our policy only takes one 2D observation image as input. Using a complementary 3D point-cloud for observation input is likely to be beneficial (Ze et al., 2024; Ling et al., 2023) for fine-grained tasks. In addition, incorporating some action primitive in the random exploration phrase, learning or defining some manipulation primitives for precise control task might also be helpful.

D Implementation Details

In this section, we describe the implementation of our proposed method and baselines.

Software: The computation platform is installed with Red Hat 7.9, Python 3.9, PyTorch 2.0, and Cuda 11.8

Hardware: For each of our experiments, we used 1 NVIDIA RTX 3090 GPU or a GPU of similar configuration.

D.1 Model Architectures

For the architecture of the video model, we adopt the same design from AVDC (Ko et al., 2023), which uses 3D UNet as video denoiser and CLIP to encode language features. In tabletop manipulation tasks, We instantiate the goal-conditioned policy by a diffusion policy (Chi et al., 2023), which use ResNet18 as image encoder and 1D UNet to denoise the action trajectory. Following the default setup in (Chi et al., 2023), we set the horizon to 16 across all other experiments. Finally, for iTHOR environment, since the action space is discrete and the required number of actions to reach goal is smaller, we use a ResNet18 with a 3-layer MLP with ReLU activation as the goal-conditioned policy with an output horizon of 1.

D.2 Training Details

Training Pipeline In training, we randomly sample sequences of image-action pairs of horizon h from the replay buffer. We provide detailed hyperparameters for training our model in Table 13 and 14. We do not apply any hyperparameter search nor learning rate scheduler. For Libero environment, the training time of our model is approximately 36 hours for a full 200k training steps. However, the performance can gradually saturate with much fewer steps, approximately within 12 hours. For the Meta-World and iThor environments, the training time of our model is approximately one day; for Calvin, the training time of our model is around 15 hours. For these environments, we also observe that the performance can gradually saturate within much less time.

Hyperparameters	Value
Horizon	16
Diffusion Time Step	100
Probability of Condition Dropout	0.2
Iterations	200K
Batch Size	64
Optimizer	Adam
Learning Rate	1e-4

Table 13: Hyperparameters of our Goal-conditioned Policy in Libero, Meta-World, and Calvin.

Hyperparameters	Value
Horizon	1
Image Encoder	ResNet18
MLP size	[(1024, 256), (256, 128), (128, 4)]
Activation	ReLu
Iterations	100K
Batch Size	64
Optimizer	Adam
Learning Rate	1e-4

Table 14: Hyperparameters of our Goal-conditioned Policy in iTHOR.

D.3 Random Action Bootstrapping Details

Random Action Bootstrapping. We provide detailed hyperparameters for random action bootstrapping in Table 15, where we use the same notations as in Section 3 and Algorithm 1.

In Table 15, # of Initial Episodes n_r and # of Addition Episodes n'_r are with respect to one task for tabletop manipulation and with respect to one scene in iTHOR navigation. In Libero, the policy learns all 8 tasks concurrently; In Meta-World, the policy learns each task separately; In Calvin, the policy learns all 4 tasks concurrently; In iTHOR, the policy learns all 4 scenes (12 tasks) concurrently. In addition, before video-guided exploration, we first warm-start the policy by training it solely on the initial random action episodes for N_r steps.

We use the *first in, first Out* convention to implement the replay buffer. The replay buffer is shared across tasks if doing multi-task exploration, thus the replay buffer size is relatively larger for multi-task setting.

	Libero	Meta-World	Calvin	iTHOR
Warm-start steps N_r	10k	10k	10k	10k
Episode Length	120	120	120	50
Action Chunk Size l_c	24	24	24	1
# of Initial Episodes n_r	50	200	100	100
Periodic Frequency q_r	500	500	500	500
# of Addition Episodes n'_r	2	10	4	2
Replay Buffer Size	1200	500	1200	1200

Table 15: Hyperparameters for Random Action Bootstrapping in each Environment. Same notations are used as in Section 3 and Algorithm 1. n_r and n'_r represent number of random action exploration per task.

In Table 16, we provide the values of a_{low} and a_{high} for sampling random actions, which are introduced in Section 3.2. For visual navigation tasks, since the action space is discrete, we sample from the four possible actions {Move Ahead, Turn Left, Turn Right, Done} with uniform probability during the random action bootstrapping.

	Libero	Meta-World	Calvin
a_{low}	[-1,-1,-1,-0.01,-0.01,-0.01]	[-1,-1,-1]	[-1,-1,-1,-1,-1,-1,-1]
a_{high}	[1,1,1,0.01,0.01,0.01]	[1,1,1]	[1,1,1,1,1,1]

Table 16: Values of a_{low} and a_{high} for Random Action Sampling. The gripper action is discretized to -1 and 1 (close and open) hence not included in the table. In Libero environment, a smaller value in the orientation action space is set for more efficient random action bootstrapping.

D.4 Task Success Metric

In this section, we describe the metric to evaluate whether a task is successfully completed. Specifically, the simulation environment will check the state of the target object in manipulation tasks or check the agent state in visual navigation tasks after executing an action. For manipulation tasks, if the target object is within the range of the specified goal state, the environment will return a success; for navigation tasks, if the target object is within a certain distance and in the view of the agent and the agent executes a 'Done' action, the environment will return a success.

During a rollout, if a success is returned, this rollout will be counted as success and terminated; otherwise, if we have finished a rollout (i.e., have sequentially executed all the synthesized video frames) and no success is returned, this episode will be counted as a failed rollout.

D.5 Implementation of Baselines

Behavior Cloning (BC). For BC, the observed image is first fed to a ResNet-18 (He et al., 2016) to encode visual information. The vision feature vector is then fed into a 3-layer MLP to predict the next action. For multi-task BC, we concatenate the vision feature with task language description feature encoded by CLIP, and feed the concatenated feature to a 3-layer MLP to predict an action. We use MSE as loss and train for 100k steps with a batch size of 64.

Diffusion Policy Behavior Cloning (DP BC). For DP BC, following (Chi et al., 2023), we use a 1D convolutional neural network as trajectory denoiser and use a ResNet-18 to encode the image observation. We set the diffusion denoising timestep to 100, horizon to 16, and train for 200k iterations with a batch size of 64.

Goal-conditioned Behavior Cloning (GCBC). For GCBC, we concatenate the start image and goal image and feed it to ResNet-18 to encode the visual observation. Similarly, the visual feature is then fed to a 3-layer MLP to predict the next action. We use MSE as loss and train for 100k steps with a batch size of 64. In test-time, given a task, similar to our proposed method, we use the same video model to generate subgoals for GCBC to complete the task.

Diffusion Policy Goal-conditioned Behavior Cloning (DP GCBC). For DP GCBC, we use an additional ResNet-18 image encoder to encode the goal image, and otherwise the model architecture is the same as DP BC. Note that the model for this baseline is also identical to the model we use in our proposed method. The goal image feature will then be concatenated with observation image features to condition the denoiser network. We set the diffusion denoising timestep to 100, horizon to 16, and train for 200k iterations with a batch size of 64.

AVDC. For AVDC, we directly adopt the official codebase (Ko et al., 2023). In Meta-world, we directly use the video model provided in the codebase, which is also the same video model for our method. In AVDC paper, the results are averaged across three different camera views, while our method only uses one camera view. Thus, for AVDC we report results on the same camera view as our method. In iTHOR, we notice that the video model resolution in the codebase is only (64, 64), which is too blurry to identify the target objects. Therefore, we train our video model with a resolution of (128, 128). Since AVDC does not experiment with Libero, we train our video model in this environment.

SuSIE. For SuSIE, we first train an image-editing diffusion model using the same video demonstration data to train the video model. The image-editing diffusion model also takes as input an observation image and a task description, but outputs the next subgoal image. We then use image-editing model to generate subgoal to guide our exploration, keeping all other hyperparameters the same.